Lattice sum for a hexagonal close-packed structure and its dependence on the c/a ratio of the hexagonal cell parameters

Antony Burrows,[1] Shaun Cooper,[2,*] and Peter Schwerdtfeger[1,†]

[1]*Centre for Theoretical Chemistry and Physics, New Zealand Institute for Advanced Study (NZIAS), Massey University Albany, Private Bag 102904, Auckland 0745, New Zealand*

[2]*School of Mathematical and Computational Sciences, Massey University Albany, Private Bag 102904, Auckland 0745, New Zealand*

(Received 13 March 2023; accepted 17 May 2023; published 8 June 2023)

We continue the work by Lennard-Jones and Ingham, and later by Kane and Goeppert-Mayer, and present a general lattice sum formula for the hexagonal close packed (hcp) structure with different c/a ratios for the two lattice parameters a and c of the hexagonal unit cell. The lattice sum is expressed in terms of fast converging series of Bessel functions. This allows us to analytically examine the behavior of a Lennard-Jones potential as a function of the c/a ratio. In contrast to the hard-sphere model, where we have the ideal ratio of $c/a = \sqrt{8/3}$ with 12 kissing spheres around a central atom, we observe the occurrence of a slight symmetry-breaking effect and the appearance of a second metastable minimum for the (12,6) Lennard-Jones potential around the ratio $c/a = 2/3$. We also show that the analytical continuation of the (n, m) Lennard-Jones potential to the domain $n, m < 3$ such as the Kratzer potential $(n = 2, m = 1)$ gives unphysical results.

DOI: 10.1103/PhysRevE.107.065302

I. INTRODUCTION

The hexagonal close packed structure (hcp) shown in Fig. 1 with a packing sequence of $(AB)_\infty$ is made up of hexagonal layers stacked in three dimensions. When the lattice parameters are in the ratio of $c/a = \sqrt{8/3}$ the hcp structure has the same packing density ($\rho = \pi/3\sqrt{2}$) as the face-centered cubic structure (fcc) with a stacking sequence of $(ABC)_\infty$. It has only recently been proven by Hales that the fcc packing density cannot be surpassed (Kepler's original conjecture [1]) and therefore is optimal [2]. Of course, any Barlow packing, which can be seen as mixtures of hcp and fcc stacking sequences, such as $(ABCBCACAB)_\infty$, is also optimal, and there are infinitely many [3–6].

In 1924 Lennard-Jones and Ingham used an inverse power-law potential of the form

$$V_{\rm LJ}(r) = \frac{\epsilon nm}{n-m}\left[\frac{1}{n}\left(\frac{r_e}{r}\right)^n - \frac{1}{m}\left(\frac{r_e}{r}\right)^m\right], \tag{1}$$

for $n > m$ ($n, m \in \mathbb{R}$ and $n, m > 3$) and lattice sums L_n in order to obtain estimates for the cohesive energies for the simple cubic (sc), body-centered cubic (bcc), and face-centered cubic (fcc) lattices [7,8],

$$E_{\rm LJ}^{\rm coh}(R) = \frac{\epsilon nm}{2(n-m)}\left[\frac{L_n}{n}\left(\frac{r_e}{R}\right)^n - \frac{L_m}{m}\left(\frac{r_e}{R}\right)^m\right]. \tag{2}$$

In the above, r_e is the equilibrium distance for the LJ potential of two interacting atoms, that is, $\frac{\partial}{\partial r}V_{\rm LJ}(r)|_{r=r_e} = 0$, and ϵ its dissociation energy, and R is a distance parameter dependent on the specific lattice. In the case of the sc, bcc, or fcc lattice, R is simply the nearest-neighbor distance $r_{\rm NN} = \min(d_{ij})$, where d_{ij} is the distance between two lattice points i and j. In our case, as we shall see, R represents the hcp lattice constant a in the solid. The potential form in (1) would later come to be commonly known as the Lennard-Jones (LJ) potential (albeit introduced earlier by Grüneisen [9]) and is one of the most widely used two-body potentials in phase simulations.

The lattice sums for the cubic lattices are infinite sums in terms of quadratic forms involving the (3×3) Gram matrix G,

$$L_n = \lambda \sum_{\vec{i}\in\mathbb{Z}^3\setminus\vec{0}} (\vec{i}^{\top} G \vec{i})^{-n/2}. \tag{3}$$

The components of G are defined by the scalar products of three lattice vectors $\vec{b}_i$ defining the Bravais lattice in question, $(G_{ij}) = (\vec{b}_i^{\top}\vec{b}_j)$, and the role of the parameter $\lambda \in \mathbb{R}_+$ will become clear later. For example, in the simple cubic lattice, G becomes simply the identity matrix, $G_{\rm sc} = I$. Such lattice sum expressions can easily be extended to higher dimensions ($N > 3$) and in principle to other types of potentials, although expressions for L_n can become rather more complicated functions of the underlying lattice [10–12]. A nice example here is the Madelung constant for dimensions up to $N = 4$ and even dimensions $N = 6$ and 8 [12,13] and more recently for any dimension N [14]. The series (3) converges for $n > 3$ and diverges otherwise.

There are many different methods to convert the usually slow convergent lattice sums for inverse power potentials into fast converging series for which a detailed account is given by Borwein *et al.* [12] Such expressions contain standard functions which allow for analytical continuation into the region ($n < 3$ for the cubic lattices) where such a series as shown in

*s.cooper@massey.ac.nz
†peter.schwerdtfeger@gmail.com

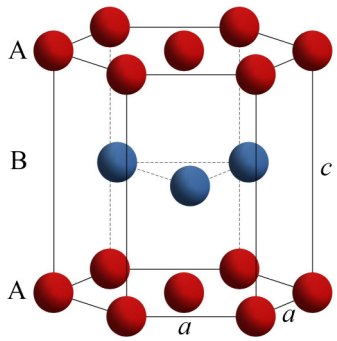

FIG. 1. The hcp structure with ABABAB... sequence (layers A in red and B in blue) of hexagonal close-packed layers and corresponding cell parameters a and c. The ratio $c/a = \sqrt{8/3}$ leads to the optimal hcp lattice with maximum packing density and 12 kissing spheres around a central atom.

(3) diverges. Some of these methods have recently been used to produce fast converging series [15] very much in the spirit of Lennard-Jones' early work on lattice sums [7,8].

In 1940 Kane and Goeppert-Mayer evaluated the lattice sum for the ideal hcp structure [16]. Although they did not provide an explicit expression for the lattice sum in their paper (which was given later by Bell and Zucker [17]), their values obtained from direct summation plus estimate of the remainder for L_n where $n = 6$, 8, 10, and 12 were accurate to four decimal places. They stated that "for the hexagonal crystal, the method used by Lennard-Jones could not easily be adopted, so we have used a more tedious and less elegant method" [16], which was by direct summation [18]. Borwein *et al.* decomposed the hcp lattice in terms of four different lattice sums containing quadratic functions but did not provide an efficient method for evaluating them [12].

Lattice sums using direct summation and their phase diagram implications for the LJ model applied to the close-packed fcc and hcp lattices have been studied by Stillinger [19]. In a recent paper [20] we introduced lattice sums for cubic lattices and the hcp structure followed by various expansion methods using Bessel functions leading to very fast convergent series thus avoiding computer time expensive and slowly converging direct summation techniques. The derived expansions for the hcp lattice were all restricted to the ideal ratio of $c/a = \sqrt{8/3}$ and were in some cases rather cumbersome. Here we introduce new and more efficient fast converging expressions for the lattice sum of the hcp structure with an arbitrary c/a ratio. We analyze the lattice in detail for the LJ potential defined in (1) and look for possible symmetry-breaking effects where the kissing number (number of touching spheres around a central atom in a lattice) of the 12 equidistant atoms from the central atom is lowered. Here we mention that recently a second metastable minimum was found in solid-state calculations using an extended LJ potential and direct lattice summations [21], and we will show that an analytical treatment using exact lattice summations, not only leads to the same metastable minimum but gives insight into why such a minimum exists. Moreover, we discuss the relationship with the fcc lattice in terms of lattice sums and analyze if analytical continuation gives physical relevant results or not.

II. THE LATTICE SUM FOR THE HEXAGONAL CLOSED PACKED STRUCTURE

A. The hexagonal Bravais lattice

Consider an inverse power potential of the form

$$V(r) = kr^{-n}. \tag{4}$$

If all atoms in a Bravais lattice interact through such a potential then the cohesive energy becomes

$$E^{\mathrm{coh}} = k \lim_{N\to\infty} \frac{1}{N} \sum_{i<j}^{N} r_{ij}^{-n} = \frac{k}{2} \lim_{N\to\infty} \frac{1}{N} \sum_{i\neq j}^{N} r_{ij}^{-n} = \frac{k}{2} \sum_{i\in\mathbb{N}} r_{0i}^{-n}, \tag{5}$$

where r_{ij} is the distance between atom i and j. For the last sum we used translational symmetry for a Bravais lattice with an arbitrarily chosen origin at the position of one of the atoms in the lattice.

For a hexagonal Bravais lattice we choose the basis vectors in the following form:

$$\vec{b}_1^{\top} = a(1, 0, 0), \quad \vec{b}_2^{\top} = a\left(\frac{1}{2}, \frac{\sqrt{3}}{2}, 0\right), \quad \vec{b}_3^{\top} = c(0, 0, 1). \tag{6}$$

This leads to the positive definite and symmetric Gram matrix

$$(G_{ij}) = (\vec{b}_i^{\top}\vec{b}_j) = a^2 \begin{pmatrix} 1 & \frac{1}{2} & 0 \\ \frac{1}{2} & 1 & 0 \\ 0 & 0 & \frac{c^2}{a^2} \end{pmatrix}, \tag{7}$$

with $\det(G) = \frac{3}{4}a^4c^2 > 0$. From our arbitrarily chosen atom at the origin, all points in the hexagonal lattice can be reached through the distance vectors

$$\vec{r}_{ijk} = i\vec{b}_1 + j\vec{b}_2 + k\vec{b}_3. \tag{8}$$

Their distances to the origin are given by the following quadratic form:

$$r_{ijk}(a, c) = |\vec{r}_{ijk}| = (\vec{v}^{\top} G \vec{v})^{\frac{1}{2}} = a\left(i^2 + ij + j^2 + \frac{c^2}{a^2}k^2\right)^{\frac{1}{2}}, \tag{9}$$

with $\vec{v}^{\top} = (i, j, k) \in \mathbb{Z}^3$ and $i, j, k \in \mathbb{Z}$ ($i = j = k = 0$ excluded). The volume of the unit cell is determined through the Gram matrix

$$V(a, c) = \sqrt{\det G} = \frac{\sqrt{3}}{2}a^2c. \tag{10}$$

The nearest-neighbor distance is then given by

$$r_{\mathrm{NN}}(a, c) = \min\{r_{ijk}\} = \min\{a, c\}. \tag{11}$$

For the following we define the parameter $\gamma = c/a > 0$, that is, we move from the original (a, c) parameter space to (a, γ). This is convenient as the lattice constant a becomes just a multiplicative constant. In other words, we do not have to carry it through in the evaluation of our lattice sum L, which then becomes dependent only on the single parameter γ. This leads to the following expression for our inverse power

potential $\sim r^{-n}$:

$$L^A(s,\gamma) = a^n \sum_{\vec{i}\in\mathbb{Z}^3\setminus\vec{0}} (\vec{v}^{\top} G \vec{v})^{-n/2} = \sum_{i,j,k\in\mathbb{Z}}{}' (i^2 + ij + j^2 + \gamma^2 k^2)^{-s} \tag{12}$$

with $s = n/2$. The λ parameter in (3) is set to $\lambda = a^n$ so that $L^A(s,\gamma)$ is dependent only on s and γ. The prime on the sum indicates that the summation is over all integers except for the term corresponding to $i = j = k = 0$. We note here that these lattice sums can be seen as special cases of the Epstein zeta function [22]. A peculiarity of this lattice sum is that $\lim_{s\to\infty} L^A(s,\gamma) = \infty$ for $\gamma < 1$, and one has to take special care of large s values in this small γ region.

B. The hcp multilattice

The hcp structure is a multilattice [23] characterized by two nested hexagonal Bravais lattices with one layer shifted by a vector of $\vec{v}_s^{\top} = a(\frac{1}{2}, \frac{1}{2\sqrt{3}}, \frac{c}{2a})$ with respect to the lattice vectors given in (6), such that the position of any atom in the B layers is given by

$$\vec{r}^{\,\mathrm{AB}}_{ijk}(a,c) = i\vec{b}_1 + j\vec{b}_2 + k\vec{b}_3 + \vec{v}_s, \tag{13}$$

with $\vec{b}_1, \vec{b}_2$, and $\vec{b}_3$ as in (6). The shift vector can easily be derived from the fact that an atom in the B layer sits above the centroid of a triangle of neighboring lattice points in the A layer. Once can also describe the hcp structure as a base hexagonal lattice introducing the middle B layer in the right (Wyckoff) positions [24] inside the Bravais lattice as shown in Fig. 1.

The corresponding lattice sum for the distances from the origin in the A layer to all points in the B layers can now easily be obtained and is given by [20]

$$L^B(s,\gamma) = \sum_{i,j,k\in\mathbb{Z}} \left[\left(i+\frac{1}{3}\right)^2 + \left(j+\frac{1}{3}\right)^2 + \left(i+\frac{1}{3}\right)\left(j+\frac{1}{3}\right) + \gamma^2\left(k+\frac{1}{2}\right)^2 \right]^{-s}, \tag{14}$$

where we also multiplied through by the parameter $\lambda = a^n$. The lattice sums (12) and (14) are exactly those given by Bell and Zucker [17]. The lattice sum $L^B(s,\gamma)$ is not a quadratic form but a quadratic function instead, which is therefore more difficult to evaluate through techniques such as the Terras decomposition [25] used in Ref. [20]. One way is to decompose $L^B(s,\gamma)$ into a sum of four lattice sums that involve quadratic forms; see Appendix D. Another way is to work with (14) directly and employ the theory of cubic theta functions, as we will see in Sec. III, where two different formulas are obtained. Again, one has to take special care of large s values for small values of γ as we have $\lim_{s\to\infty} L^B(s,\gamma) = \infty$ for $\gamma < \sqrt{\frac{8}{3}}$.

Taking both AB layers into account the lattice sum for the hexagonal close packed structure is given by

$$L^{\mathrm{hcp}}(s,\gamma) = L^A(s,\gamma) + L^B(s,\gamma). \tag{15}$$

For the nearest-neighbor distance r_{NN} in an hcp lattice we have to also consider the neighboring distance between points in the A and B layers, and so

$$r_{\mathrm{NN}}(a,\gamma) = \min\left\{a, c, \sqrt{\frac{a^2}{3} + \frac{c^2}{4}}\right\} = a\min\left\{1, \gamma, \sqrt{\frac{1}{3} + \frac{1}{4}\gamma^2}\right\} = a\begin{cases}\gamma & \text{if } 0 < \gamma \leqslant \frac{2}{3} \\ \sqrt{\frac{1}{3} + \frac{\gamma^2}{4}} & \text{if } \frac{2}{3} < \gamma < \sqrt{\frac{8}{3}} \\ 1 & \text{if } \gamma \geqslant \sqrt{\frac{8}{3}}.\end{cases} \tag{16}$$

To compute the density, we have from (10) that the volume of a cell in the hexagonal lattice is

$$V = \frac{\sqrt{3}}{2}a^2 c = \frac{\sqrt{3}}{2}a^3\gamma. \tag{17}$$

Insertion of the B layer means that each cell contains two atoms and therefore halves the occupied volume, and hence for cells in the hcp lattice we have

$$V_{\mathrm{cell}} = \frac{1}{2} \times \frac{\sqrt{3}}{2}a^2 c = \frac{\sqrt{3}}{4}a^3\gamma. \tag{18}$$

The volume of a sphere is given by

$$V_{\mathrm{sphere}} = \frac{4}{3}\pi\left(\frac{r_{\mathrm{NN}}(a,\gamma)}{2}\right)^3, \tag{19}$$

and therefore the density of the lattice is given by

$$\rho(\gamma) = \frac{V_{\mathrm{sphere}}}{V_{\mathrm{cell}}} = \frac{2\pi}{3\sqrt{3}} \times \frac{1}{\gamma} \times \left(\frac{r_{\mathrm{NN}}(a,\gamma)}{a}\right)^3 = \begin{cases} \frac{2\pi}{3\sqrt{3}}\gamma^2 & \text{if } 0 < \gamma \leqslant \frac{2}{3}, \\ \frac{2\pi}{3\sqrt{3}} \times \frac{1}{\gamma}\left(\frac{1}{3} + \frac{\gamma^2}{4}\right)^{3/2} & \text{if } \frac{2}{3} < \gamma < \sqrt{\frac{8}{3}}, \\ \frac{2\pi}{3\sqrt{3}} \times \frac{1}{\gamma} & \text{if } \gamma \geqslant \sqrt{\frac{8}{3}}. \end{cases} \tag{20}$$

Graphs of the density $\rho(\gamma)$ and the normalized nearest-neighboring distance $a^{-1}r_{\mathrm{NN}}(a,\gamma)$ as functions of γ are shown in Fig. 2. For hard unit spheres there is also a requirement that $r_{\mathrm{NN}}(1,\gamma) \geqslant 1$, and this gives the condition that $\gamma \geqslant \sqrt{8/3}$, corresponding to the region labeled III in Fig. 2.

The optimal packing density occurs when $\gamma = \sqrt{\frac{8}{3}}$ and is given by

$$\rho\left(\sqrt{\frac{8}{3}}\right) = \frac{\pi}{3\sqrt{2}} = 0.74048048969\ldots, \tag{21}$$

identical to that of the fcc lattice [1,2]. The value $\gamma = \sqrt{\frac{8}{3}}$ corresponds to the hexagonal close packing structure. The kissing number is $\kappa = 12$.

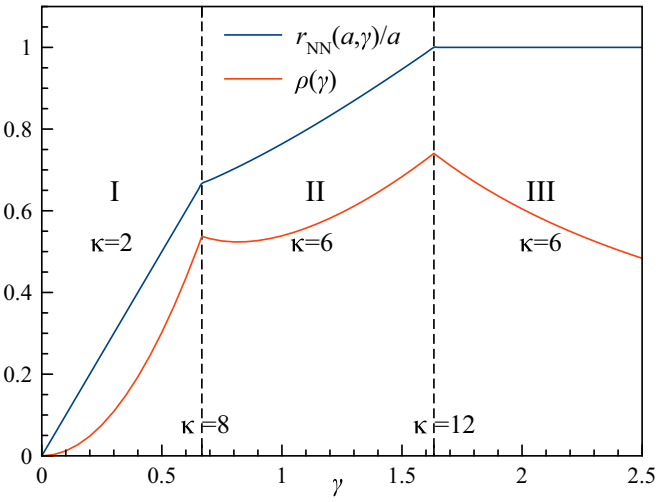

FIG. 2. Normalized nearest-neighbor distance $r_{NN}(a,\gamma)/a$ according to Eq. (16) and the optimal packing density $\rho(\gamma)$ according to Eq. (21). The kissing number κ for the three regions and at the two boundaries are shown. The vertical dashed lines are at $\gamma = \frac{2}{3}$ and $\sqrt{\frac{8}{3}}$ where we have increased kissing numbers.

III. BESSEL FUNCTION EXPANSIONS OF THE HCP LATTICE SUM

In the following we analyze $L^A(s)$ and $L^B(s)$ one at a time (we omit the argument γ for better clarity). We obtain two different Bessel function expansions which have poles at different s values (except for $s = 3/2$) and thus can be used to check against each other. In the proofs we will frequently refer to formulas for special functions given by (A1)–(A25) in Appendix A.

A. The lattice sum $L^A(s)$

We break the sum for $L^A(s)$ into two, according to whether $k = 0$ or $k \neq 0$. This gives

$$L^A(s) = f(s) + 2F(s), \tag{22}$$

where

$$f(s) = {\sum_{i,j\in\mathbb{Z}}}' (i^2 + ij + j^2)^{-s} \tag{23}$$

and

$$F(s) = \sum_{k\in\mathbb{N}} \sum_{i,j\in\mathbb{Z}} (i^2 + ij + j^2 + \gamma^2 k^2)^{-s}, \tag{24}$$

with $\mathbb{N}$ defined as the set of positive integers, and $\mathbb{N}_0$ includes the zero. The function $f(s)$ has been evaluated before [12,26],

$$f(s) = 6\zeta(s) L_{-3}(s) = 3^{1-s} 2\zeta(s)\left[\zeta\left(s, \tfrac{1}{3}\right) - \zeta\left(s, \tfrac{2}{3}\right)\right], \tag{25}$$

where $\zeta(s,x)$ is the Hurwitz zeta function

$$\zeta(s,x) = \sum_{i\in\mathbb{N}_0} (i+x)^{-s}, \tag{26}$$

where $\zeta(s) = \zeta(s,1)$ is the Riemann zeta function, and L_{-3} is the L function defined by

$$L_{-3}(s) = \sum_{k\in\mathbb{N}} \frac{\sin(2k\pi/3)}{\sin(2\pi/3)} \frac{1}{k^s} = \frac{1}{1^s} - \frac{1}{2^s} + \frac{1}{4^s} - \frac{1}{5^s} + \cdots. \tag{27}$$

It remains to calculate $F(s)$. Applying the gamma function integral shown in (A2),

$$\frac{1}{w^s} = \frac{1}{\Gamma(s)} \int_{[0,\infty)} x^{s-1} e^{-wx}\, dx, \tag{28}$$

followed by the cubic analog of the theta function transformation formula, (A12), we obtain

$$\begin{aligned}(2\pi)^{-s}\Gamma(s)F(s) &= \int_{[0,\infty)} x^{s-1} \sum_{k\in\mathbb{N}} e^{-2\pi\gamma^2k^2x} \sum_{i,j\in\mathbb{Z}} e^{-2\pi(i^2+ij+j^2)x}\, dx \\ &= \frac{1}{\sqrt{3}} \int_{[0,\infty)} x^{s-2} \sum_{k\in\mathbb{N}} e^{-2\pi\gamma^2k^2x} \sum_{i,j\in\mathbb{Z}} e^{-2\pi(i^2+ij+j^2)/3x}\, dx.\end{aligned} \tag{29}$$

Now separating out the $i = j = 0$ term and evaluate the resulting integrals using the following expression for the modified Bessel functions of the second kind shown in (A3)

$$\int_{[0,\infty)} x^{s-1} e^{-ax-b/x}\, dx = 2\left(\frac{b}{a}\right)^{s/2} K_s(2\sqrt{ab}), \tag{30}$$

we get

$$\begin{aligned}(2\pi)^{-s}\Gamma(s)F(s) &= \frac{1}{\sqrt{3}} \sum_{k\in\mathbb{N}} \int_{[0,\infty)} x^{s-2} e^{-2\pi\gamma^2k^2x}\, dx + \frac{1}{\sqrt{3}} \sum_{k\in\mathbb{N}} {\sum_{i,j\in\mathbb{Z}}}' \int_{[0,\infty)} x^{s-2} e^{-2\pi\gamma^2k^2x - 2\pi(i^2+ij+j^2)/3x}\, dx \\ &= \frac{(2\pi\gamma^2)^{1-s}}{\sqrt{3}} \Gamma(s-1)\zeta(2s-2) + \frac{2}{\sqrt{3}} \sum_{k\in\mathbb{N}} {\sum_{i,j\in\mathbb{Z}}}' \left(\frac{i^2+ij+j^2}{3\gamma^2k^2}\right)^{(s-1)/2} K_{s-1}\left(\frac{4\pi}{\sqrt{3}}\gamma k\sqrt{i^2+ij+j^2}\right).\end{aligned} \tag{31}$$

It follows that

$$\begin{aligned}L^A(s) &= 6\zeta(s)L_{-3}(s) + \frac{4\pi}{\sqrt{3}(s-1)}\gamma^{2-2s}\zeta(2s-2) + \frac{4}{\sqrt{3}}\frac{(2\pi)^s}{\Gamma(s)} \sum_{k\in\mathbb{N}} {\sum_{i,j\in\mathbb{Z}}}' \left(\frac{i^2+ij+j^2}{3\gamma^2k^2}\right)^{(s-1)/2} K_{s-1}\left(\frac{4\pi}{\sqrt{3}}\gamma k\sqrt{(i^2+ij+j^2)}\right) \\ &= 6\zeta(s)L_{-3}(s) + \frac{4\pi}{\sqrt{3}(s-1)}\gamma^{2-2s}\zeta(2s-2) + \frac{4}{\sqrt{3}}\frac{(2\pi)^s}{\Gamma(s)} \sum_{k\in\mathbb{N}} \sum_{N\in\mathbb{N}} u_2(N) \left(\frac{N}{3\gamma^2k^2}\right)^{(s-1)/2} K_{s-1}\left(\frac{4\pi}{\sqrt{3}}\gamma k\sqrt{N}\right),\end{aligned} \tag{32}$$

where $u_2(N)$ is the number of representations of N by the form $i^2 + ij + j^2$.

B. A second formula for the lattice sum $L^A(s)$

A different formula for $L^A(s)$ can be obtained by separating the terms in the series (12) according to whether $i = j = 0$ or i and j are not both zero. This gives

$$L^A(s) = 2\gamma^{-2s}\zeta(2s) + G(s), \tag{33}$$

where

$$G(s) = {\sum_{i,j\in\mathbb{Z}}}' \sum_{k\in\mathbb{Z}} (i^2 + ij + j^2 + \gamma^2 k^2)^{-s}. \tag{34}$$

Applying the gamma function integral (A2) followed by the theta function transformation formula (A8) for the k summation, we obtain

$$\begin{aligned}\pi^{-s}\Gamma(s)G(s) &= \int_{[0,\infty)} x^{s-1} {\sum_{i,j\in\mathbb{Z}}}' e^{-\pi(i^2+ij+j^2)x} \sum_{k\in\mathbb{Z}} e^{-\pi\gamma^2k^2x}\,dx \\ &= \gamma^{-1}\int_{[0,\infty)} x^{s-\frac{3}{2}} {\sum_{i,j\in\mathbb{Z}}}' e^{-\pi(i^2+ij+j^2)x} \sum_{k\in\mathbb{Z}} e^{-\pi k^2/(\gamma^2x)}\,dx.\end{aligned} \tag{35}$$

Now separate out the $k = 0$ term and evaluate the resulting integrals. The result is

$$\begin{aligned}\pi^{-s}\Gamma(s)G(s) &= \gamma^{-1}\int_{[0,\infty)} x^{s-\frac{3}{2}} {\sum_{i,j\in\mathbb{Z}}}' e^{-\pi(i^2+ij+j^2)x}\,dx + 2\gamma^{-1}\int_{[0,\infty)} x^{s-\frac{3}{2}} {\sum_{i,j\in\mathbb{Z}}}' e^{-\pi(i^2+ij+j^2)x} \sum_{k\in\mathbb{N}} e^{-\pi k^2/(\gamma^2x)}\,dx \\ &= \gamma^{-1}\pi^{-(s-\frac{1}{2})}\,\Gamma\left(s-\frac{1}{2}\right) {\sum_{i,j\in\mathbb{Z}}}' (i^2+ij+j^2)^{-s+\frac{1}{2}} + 4\gamma^{-(2s+1)/2} {\sum_{i,j\in\mathbb{Z}}}' \sum_{k\in\mathbb{N}} \left(\frac{k^2}{i^2+ij+j^2}\right)^{(2s-1)/4} \\ &\quad \times K_{s-\frac{1}{2}}\left(\frac{2\pi k}{\gamma}\sqrt{i^2+ij+j^2}\right).\end{aligned} \tag{36}$$

The first sum can be evaluated in terms of the Riemann zeta function and the L_{-3} function by (A24). In the second sum, we again use the notation $u_2(N)$ for the number of representations of N by the form $i^2 + ij + j^2$. The result is

$$\begin{aligned}\pi^{-s}\Gamma(s)G(s) &= 6\,\pi^{-(s-\frac{1}{2})}\,\gamma^{-1}\Gamma\left(s-\frac{1}{2}\right)\zeta\left(s-\frac{1}{2}\right)L_{-3}\left(s-\frac{1}{2}\right) \\ &\quad + 4\gamma^{-(2s+1)/2} \sum_{N\in\mathbb{N}} \sum_{k\in\mathbb{N}} u_2(N)\left(\frac{k^2}{N}\right)^{(2s-1)/4} K_{s-\frac{1}{2}}\left(\frac{2\pi k}{\gamma}\sqrt{N}\right).\end{aligned} \tag{37}$$

It follows that

$$\begin{aligned}L^A(s) &= 2\gamma^{-2s}\zeta(2s) + 6\sqrt{\pi}\gamma^{-1}\,\frac{\Gamma\left(s-\frac{1}{2}\right)}{\Gamma(s)}\,\zeta\left(s-\frac{1}{2}\right)L_{-3}\left(s-\frac{1}{2}\right) \\ &\quad + \frac{4\pi^s}{\Gamma(s)}\,\gamma^{-(2s+1)/2} \sum_{N\in\mathbb{N}} \sum_{k\in\mathbb{N}} u_2(N)\left(\frac{k^2}{N}\right)^{(2s-1)/4} K_{s-\frac{1}{2}}\left(\frac{2\pi k}{\gamma}\sqrt{N}\right).\end{aligned} \tag{38}$$

C. The lattice sum $L^B(s)$

We apply the gamma function integral (A2) for (14) to write

$$L^B(s) = \frac{(2\pi)^s}{\Gamma(s)}\int_{[0,\infty)} x^{s-1} \sum_{k\in\mathbb{Z}} e^{-2\pi\gamma^2(k+\frac{1}{2})^2x} \sum_{i,j\in\mathbb{Z}} e^{-2\pi[(i+\frac{1}{3})^2+(i+\frac{1}{3})(j+\frac{1}{3})+(j+\frac{1}{3})^2]x}\,dx. \tag{39}$$

Now make use of the transformation formula (A13) to deduce

$$L^B(s) = \frac{(2\pi)^s}{\Gamma(s)}\int_{[0,\infty)} x^{s-1}\left(2\sum_{k\in\mathbb{N}_0} e^{-2\pi\gamma^2(k+\frac{1}{2})^2x}\right)\left(\frac{1}{x\sqrt{3}}\sum_{i,j\in\mathbb{Z}} \omega^{i-j} e^{-2\pi(i^2+ij+j^2)/3x}\right)dx, \tag{40}$$

where $\omega = \exp(2\pi i/3)$ is a primitive cube root of 1. Now separate the term $i = j = 0$ to deduce

$$L^B(s) = \frac{(2\pi)^s}{\Gamma(s)}\frac{2}{\sqrt{3}}\int_{[0,\infty)} x^{s-2}\sum_{k\in\mathbb{N}_0} e^{-2\pi\gamma^2(k+\frac{1}{2})^2 x}\,dx$$
$$+\frac{(2\pi)^s}{\Gamma(s)}\frac{2}{\sqrt{3}}\int_{[0,\infty)} x^{s-2}\sum_{k\in\mathbb{N}_0} e^{-2\pi\gamma^2(k+\frac{1}{2})^2 x}\sum_{N\in\mathbb{N}}\cos\left(\frac{2\pi N}{3}\right)u_2(N)\,e^{-2\pi N/3x}\,dx, \tag{41}$$

where $u_2(N)$ is the number of representations of N by the form i^2+ij+j^2, as before. Here we used Euler's formula, $e^{i\theta} = \cos\theta + i\sin\theta$ and retain only the real part as $L^B(s)$ is real. On evaluating the integrals using (A2) and (A3) we obtain

$$L^B(s) = \frac{4\pi}{\sqrt{3}(s-1)}\gamma^{-2s+2}\sum_{k\in\mathbb{N}_0}\frac{1}{\left(k+\frac{1}{2}\right)^{2s-2}} + \frac{4}{\sqrt{3}}\frac{(2\pi)^s}{\Gamma(s)}\sum_{k\in\mathbb{N}_0}\sum_{N\in\mathbb{N}}\cos\left(\frac{2\pi N}{3}\right)$$
$$\times u_2(N)\left(\frac{N}{3\gamma^2\left(k+\frac{1}{2}\right)^2}\right)^{(s-1)/2} K_{s-1}\left(\frac{4\pi}{\sqrt{3}}\gamma\left(k+\frac{1}{2}\right)\sqrt{N}\right). \tag{42}$$

The first sum can be evaluated in terms of the Riemann zeta function by using (A23) to give

$$L^B(s) = \frac{4\pi}{\sqrt{3}(s-1)}\gamma^{-2s+2}(2^{2s-2}-1)\zeta(2s-2) + \frac{4}{\sqrt{3}}\frac{(2\pi)^s}{\Gamma(s)}\sum_{k\in\mathbb{N}_0}\sum_{N\in\mathbb{N}}\cos\left(\frac{2\pi N}{3}\right)$$
$$\times u_2(N)\left(\frac{N}{3\gamma^2(k+\frac{1}{2})^2}\right)^{(s-1)/2} K_{s-1}\left(\frac{4\pi}{\sqrt{3}}\gamma\left(k+\frac{1}{2}\right)\sqrt{N}\right). \tag{43}$$

D. A second formula for the sum $L^B(s)$

We introduce the abbreviation

$$Y_{ij} = \left(i+\tfrac{1}{3}\right)^2 + \left(i+\tfrac{1}{3}\right)\left(j+\tfrac{1}{3}\right) + \left(j+\tfrac{1}{3}\right)^2 \tag{44}$$

to write (39) in the form

$$L^B(s) = \frac{(2\pi)^s}{\Gamma(s)}\int_{[0,\infty)} x^{s-1}\sum_{i,j\in\mathbb{Z}} e^{-2\pi Y_{ij}x}\sum_{k\in\mathbb{Z}} e^{-2\pi\gamma^2(k+\frac{1}{2})^2 x}\,dx. \tag{45}$$

This time we apply the transformation formula (A9) to the sum over k to obtain

$$L^B(s) = \frac{(2\pi)^s}{\sqrt{2}\Gamma(s)}\gamma^{-1}\int_{[0,\infty)} x^{s-3/2}\sum_{i,j\in\mathbb{Z}} e^{-2\pi Y_{ij}x}\sum_{k\in\mathbb{Z}}(-1)^k\,e^{-\pi k^2/(2\gamma^2 x)}\,dx. \tag{46}$$

Now separate the terms according to whether $k = 0$ or $k \neq 0$ and evaluate the resulting integrals by (A2) and (A3). The result is

$$L^B(s) = \frac{\sqrt{\pi}\,\Gamma\left(s-\frac{1}{2}\right)}{\gamma\,\Gamma(s)}\sum_{i,j\in\mathbb{Z}} Y_{ij}^{1/2-s} + \frac{4\pi^s}{\Gamma(s)}\gamma^{-(2s+1)/2}\sum_{k\in\mathbb{N}}(-1)^k\sum_{i,j\in\mathbb{Z}}\left(\frac{k}{\sqrt{Y_{ij}}}\right)^{s-\frac{1}{2}} K_{s-\frac{1}{2}}\left(2\pi\frac{k}{\gamma}\sqrt{Y_{ij}}\right). \tag{47}$$

The first sum can be handled by (A25) to give

$$\sum_{i,j\in\mathbb{Z}} Y_{ij}^{1/2-s} = 3(3^{s-1/2}-1)\zeta\left(s-\frac{1}{2}\right)L_{-3}\left(s-\frac{1}{2}\right). \tag{48}$$

For the other sum, observe that $3Y_{ij} = 3i^2+3ij+3j^2+3i+3j+1$, that is to say $3Y_{ij}$ is a positive integer and $3Y_{ij} \equiv 1 \pmod 3$. Therefore we set $3Y_{ij} = 3N+1$ and use (A16) to deduce that the number of solutions of $3i^2+3ij+3j^2+3i+3j+1 = 3N+1$ is equal to $\frac{1}{2}u_2(3N+1)$, and we get

$$L^B(s) = \frac{3\sqrt{\pi}\,\Gamma\left(s-\frac{1}{2}\right)}{\gamma\,\Gamma(s)}\left(3^{s-1/2}-1\right)\zeta\left(s-\frac{1}{2}\right)L_{-3}\left(s-\frac{1}{2}\right)$$
$$+\frac{2\pi^s}{\Gamma(s)}\gamma^{-(2s+1)/2}\sum_{k\in\mathbb{N}}(-1)^k\sum_{N\in\mathbb{N}_0} u_2(3N+1)\left(\frac{k}{\sqrt{N+\frac{1}{3}}}\right)^{s-\frac{1}{2}} K_{s-\frac{1}{2}}\left(2\pi\frac{k}{\gamma}\sqrt{N+\frac{1}{3}}\right). \tag{49}$$

E. Adding $L^A(s)$ and $L^B(s)$

On adding the results for $L^A(s)$ and $L^B(s)$ in (32) and (43) we obtain

$$L^{\rm hcp}(s,\gamma) = 6\zeta(s)L_{-3}(s) + \frac{4\pi}{\sqrt{3}(s-1)}\left(\frac{\gamma}{2}\right)^{2-2s}\zeta(2s-2) + \frac{4}{\sqrt{3}}\frac{(2\pi)^s}{\Gamma(s)}\sum_{k\in\mathbb{N}}\sum_{N\in\mathbb{N}} u_2(N)\left(\frac{N}{3\gamma^2k^2}\right)^{(s-1)/2} K_{s-1}\left(\frac{4\pi}{\sqrt{3}}\gamma k\sqrt{N}\right)$$
$$+ \frac{4}{\sqrt{3}}\frac{(2\pi)^s}{\Gamma(s)}\sum_{k\in\mathbb{N}_0}\sum_{N\in\mathbb{N}} \cos\left(\frac{2\pi N}{3}\right) u_2(N)\left(\frac{N}{3\gamma^2\left(k+\frac{1}{2}\right)^2}\right)^{(s-1)/2} K_{s-1}\left(\frac{4\pi}{\sqrt{3}}\gamma\left(k+\frac{1}{2}\right)\sqrt{N}\right). \tag{50}$$

On the other hand, if we add the results of (38) and (49) we obtain

$$L^{\rm hcp}(s,\gamma) = 2\gamma^{-2s}\zeta(2s) + \frac{3\sqrt{\pi}\,\Gamma\left(s-\frac{1}{2}\right)}{\gamma\,\Gamma(s)}\left(3^{s-1/2}+1\right)\zeta\left(s-\frac{1}{2}\right)L_{-3}\left(s-\frac{1}{2}\right)$$
$$+ \frac{4\pi^s}{\Gamma(s)}\gamma^{-(2s+1)/2}\sum_{N\in\mathbb{N}}\sum_{k\in\mathbb{N}} u_2(N)\left(\frac{k}{\sqrt{N}}\right)^{(2s-1)/2} K_{s-\frac{1}{2}}\left(\frac{2\pi k}{\gamma}\sqrt{N}\right)$$
$$+ \frac{2\pi^s}{\Gamma(s)}\gamma^{-(2s+1)/2}\sum_{k\in\mathbb{N}}(-1)^k\sum_{N\in\mathbb{N}_0} u_2(3N+1)\left(\frac{k}{\sqrt{N+\frac{1}{3}}}\right)^{s-\frac{1}{2}} K_{s-\frac{1}{2}}\left(2\pi\frac{k}{\gamma}\sqrt{N+\frac{1}{3}}\right). \tag{51}$$

Equation (51) is numerically more stable for small values of γ as the argument in the Bessel function $K_{s-\frac{1}{2}}(x)$ becomes larger and therefore further away from the singularity at $x=0$, while (50) is better suited for larger values of γ. The lattice sums as a function of γ for different s values are shown in Fig. 3, and the corresponding values of $L^{\rm hcp}(s,\gamma)$ (including the first and second derivatives) for the ideal ratio of $\gamma_{\rm hcp}=\sqrt{\frac{8}{3}}$ and selected s values are collected in Table I.

We obtain the following limits for all values of $s > \frac{3}{2}$:

$$\lim_{\gamma\to\infty} L^{\rm hcp}(s,\gamma) = 6\zeta(s)L_{-3}(s) \quad \text{and} \quad \lim_{\gamma\to 0} L^{\rm hcp}(s,\gamma) = \infty. \tag{52}$$

The first limit reflects the fact that the limiting case $\gamma\to\infty$ corresponds to a single 2D hexagonal lattice with $L_2^{\rm hex}(s) = 6\zeta(s)L_{-3}(s)$ being the corresponding lattice sum [see Eq. (47) in Ref. [27]]. From this we get $\lim_{s\to\infty} L_2^{\rm hex}(s) = 6$ and at the pole $L_2^{\rm hex}(s=\frac{3}{2}) = 11.03417573491\ldots$. Moreover, as mentioned before we have $\lim_{s\to\infty} L^{\rm hcp}(s,\gamma)=\infty$ for $\gamma < \sqrt{\frac{8}{3}}$, and for larger values of s direct summation using the original lattice sum (15) is to be preferred, e.g., for $s=50$ and $\gamma=\gamma_{\rm hcp}=\sqrt{\frac{8}{3}}$ we obtain $L^{\rm hcp}(s,\gamma) = L^{\rm hcp}(50,\sqrt{\frac{8}{3}}) = 12.000000000000$, corresponding to the kissing number for an ideal hcp lattice. We note that the curve for $s=2$ in Fig. 3 very slowly approaches the limit $\gamma\to\infty$ of $6\zeta(2)L_{-3}(2) = 7.7111457329049\ldots$as expected for a soft and long-range potential of the form $V(r)=r^{-4}$.

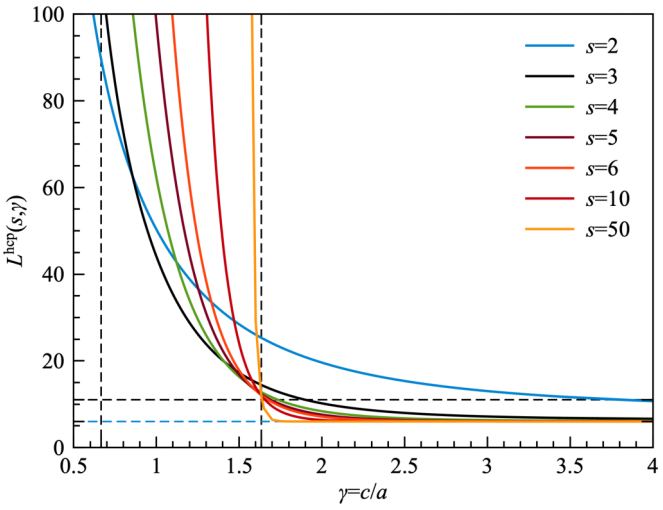

FIG. 3. Lattice sums $L^{\rm hcp}(s,\gamma)$ as a function of γ for various s values. The vertical dashed lines are at $\gamma=\frac{2}{3}$ and $\sqrt{\frac{8}{3}}$ as in Fig. 2, and the horizontal dashed line represents the two limits at large γ values, $\lim_{s\to\infty}(\lim_{\gamma\to\infty} L^{\rm hcp}(s,\gamma)) = 6$ and $\lim_{s\to 3/2}(\lim_{\gamma\to\infty} L^{\rm hcp}(s)) = 11.03417573491\ldots$. The curve for $s=50$ is close to the hard-sphere limit of $s=\infty$.

TABLE I. Values for $L^{\rm hcp}(s,\gamma)$ at the ideal ratio of $c/a=\gamma_{\rm hcp}=\sqrt{\frac{8}{3}}$ for selected $s=n/2$. The first and second derivatives with respect to γ are reported as well (see Appendix C for details).

s	$L^{\rm hcp}(s,\gamma)$	$\partial L^{\rm hcp}(s,\gamma)/\partial\gamma$	$\partial^2 L^{\rm hcp}(s,\gamma)/\partial\gamma^2$
2	25.339082338055	−20.695008216087	34.645562350540
3	14.454897277842	−17.711026910386	45.197828381987
4	12.802821852810	−20.913971214589	71.283006314719
5	12.311896233819	−25.136976828849	106.83160316772
6	12.132293769099	−29.721546123728	151.03829753868
7	12.059228255068	−34.464287703815	203.59375072251
8	12.027479419304	−39.282788797012	264.34146680290
9	12.013060023177	−44.139430042060	333.19696813736
10	12.006309158115	−49.015864608041	410.11367485711

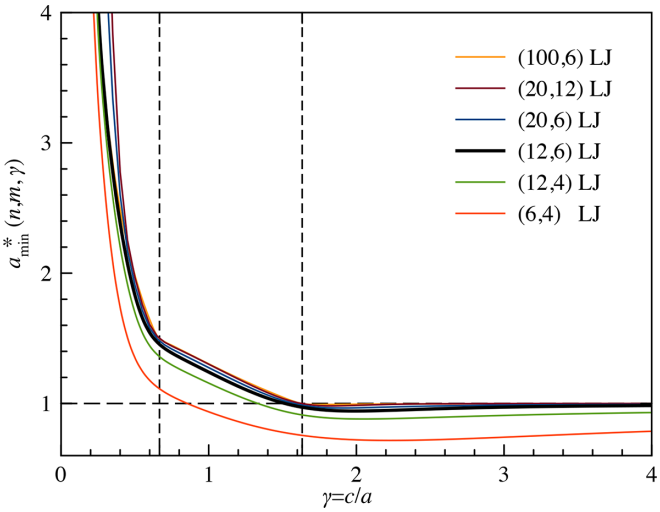

FIG. 4. The lattice parameter $a^*_{\min}(n, m, \gamma)$ for the LJ potential for selected values of n and m.

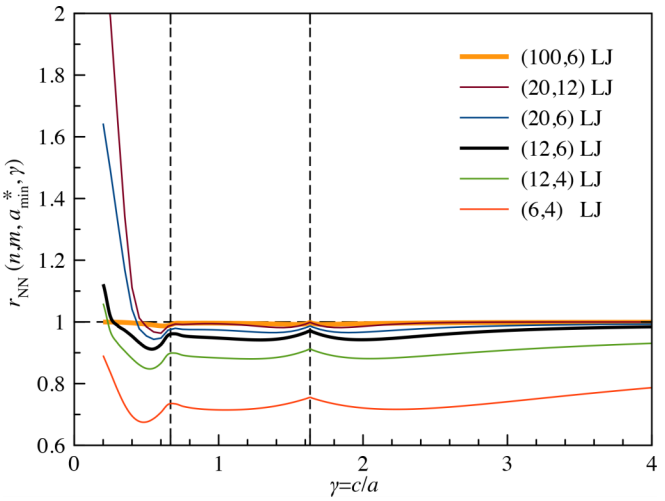

FIG. 5. The nearest-neighbor distance $r_{\rm NN}(a^*_{\min}, \gamma)$ for the LJ potential for selected values of n and m.

IV. THE LENNARD-JONES COHESIVE ENERGY FOR THE HCP STRUCTURE WITH VARYING c/a RATIO

A. Independent (a, γ) parameter space

The cohesive energy for the hcp structure for a general (n, m) LJ potential expressed in terms of lattice sums is given by

$$E^{\rm coh}_{\rm LJ}(n,m,a,\gamma)=\frac{\epsilon nm}{2(n-m)}\left[\frac{L^{\rm hcp}\left(\frac{n}{2},\gamma\right)}{n}\left(\frac{r_e}{a}\right)^n-\frac{L^{\rm hcp}\left(\frac{m}{2},\gamma\right)}{m}\left(\frac{r_e}{a}\right)^m\right]. \tag{53}$$

In the following we regard the two parameters (a, γ) as independent freely variable parameters with $a > 0$ and $\gamma > 0$. This is an approximation as we also have to consider the a dependence of $\gamma = c/a$. As we shall see, we obtain simple equations for the cohesive energy dependence on γ. A more detailed analysis and justification for this approximation will follow in the next section.

The definitions for the lattice sums $L^{\rm hcp}(s, \gamma)$ are taken from Eqs. (50) and (51). In order to discuss the behavior for the LJ potential with varying γ we calculate the minimum cohesive energy with respect to the lattice parameter a for a fixed γ value. For this we follow the procedure in Ref. [28] and get from $\partial E^{\rm coh}_{\rm LJ}/\partial a = 0$ the minimum lattice parameter,

$$a^*_{\min}(n,m,\gamma)=\frac{a_{\min}(\gamma)}{r_e}=\left(\frac{L^{\rm hcp}\left(\frac{n}{2},\gamma\right)}{L^{\rm hcp}\left(\frac{m}{2},\gamma\right)}\right)^{\frac{1}{n-m}}, \tag{54}$$

and the asterisk indicates reduced (or dimensionless) units are used. Figure 4 shows the $a^*_{\min}(n, m, \gamma)$ curve for selected values of n and m. We clearly see the steep increase in $a^*_{\min}(n, m, \gamma)$ for small values of γ. However, it might be interesting to compare to the nearest-neighbor distance (16), which is shown in Fig. 5. Only for very soft values we get $r_{\rm NN} \ll 1$. For the (100,6)-LJ potential, which is close to the hard-sphere limit, the nearest-neighbor distance stays close to 1.0 for all γ values. Moreover, at the critical point $\gamma = \sqrt{\frac{8}{3}}$ and $\gamma = \frac{2}{3}$ we have a nonsmooth behavior in $r_{\rm NN}$ as already shown in Fig. 2. We also note the minimum in $r_{\rm NN}$ at values $\gamma < \frac{2}{3}$ indicating some extra stability of this lattice, which will be discussed in the following.

The cohesive energy at $a^*_{\min}$ is given by

$$E^*_{nm}(\gamma)=E^{\rm coh}_{\rm LJ}(n,m,a^*_{\min}(\gamma),\gamma)/\epsilon=-\frac{1}{2}\left[\frac{L^{\rm hcp}\left(\frac{m}{2},\gamma\right)^n}{L^{\rm hcp}\left(\frac{n}{2},\gamma\right)^m}\right]^{\frac{1}{n-m}}. \tag{55}$$

The function $E^*_{nm}(\gamma)$ is shown in Fig. 6 for various (n, m) combinations of the LJ potential. For the (12,6) LJ potential we see a metastable minimum around $\gamma = 2/3$

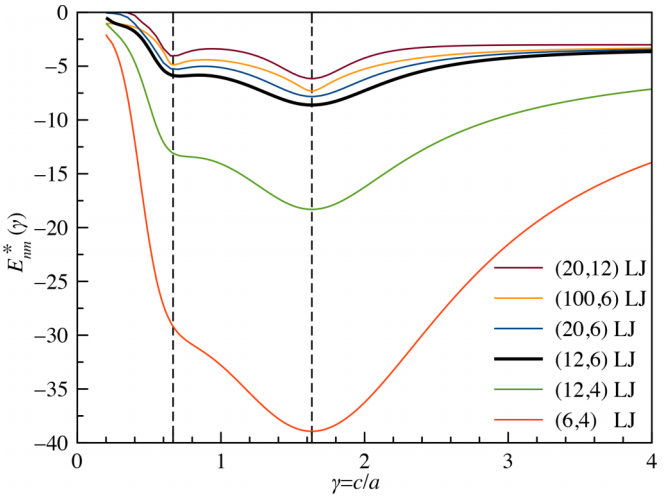

FIG. 6. $E^*_{nm}(\gamma)$ as a function of $\gamma = \frac{c}{a}$ at $a^*_{\min}$ for a number of (n, m) combinations for the LJ potential. The vertical dashed lines are at $\gamma = \frac{2}{3}$ and $\sqrt{\frac{8}{3}}$ as in Fig. 2. Note that the exponents n, m are multiplied by 2 compared to the s exponent used in the previous sections.

TABLE II. $\gamma_{\min}^{\text{meta}}$ for the metastable minimum and corresponding energy difference ΔE_{nm}^{*} to the global minimum (around $\gamma_{\text{hcp}} = \sqrt{\frac{8}{3}}$ and $\gamma_{\max}$ between the two minima and corresponding energy difference $\Delta E_{nm}^{*\,\#}$ to the metastable minimum for three selected (n, m) combinations of the LJ potential. Note that the exponents n, m are multiplied by 2 compared to the s exponent used in the previous sections.

n	m	$\gamma_{\min}^{\text{meta}}$	$\gamma_{\max}$	ΔE_{nm}^{*}	$\Delta E_{nm}^{*\,\#}$
12	6	0.710188	0.848360	2.691402	0.08449406
20	6	0.683350	0.883096	2.519636	0.29600569
20	12	0.668678	0.935797	2.073051	0.70435894

($\gamma = 0.710188$ for the (12,6) LJ potential with an energy difference to the global minimum of $\Delta E^{*} = 2.691401$. The metastable minimum becomes more pronounced for harder potentials and disappears for very soft potentials. Concerning the maximum, for the (12,6) LJ potential it sits at $\gamma = 0.848360$ with an activation barrier of $\Delta E^{*} = 0.084494$ from the metastable minimum to the more stable minimum around $\gamma_{\text{hcp}} = \sqrt{\frac{8}{3}}$. Data for the metastable minimum for some other (n, m) combinations of the LJ potential are collected in Table II.

The question why a second minimum appears around $\gamma = \frac{2}{3}$ needs to be addressed. This is at the boundary between regions I and II shown in Fig. 2 where the kissing number is increased to $\kappa = 8$ due to the fact that beside the six surrounding atoms from the A layer of an atom in the B layer, we have two more touching spheres above and below from other C layers with an underlying elongated triangular bipyramid (or dipyramid). In region I, the nearest-neighbor distance is determined by the lattice constant c. In this case the atoms in the two A layers shown in Fig. 1 come in direct neighborhood and start to interact more strongly. In order to avoid strong repulsive forces we have to make space for the C layer in the middle position by increasing the lattice constant a. As an atom in layer C sits exactly in the centroid of a triangle spanned by neighboring atoms in the A layer, we consider a trigonal pyramid of unit spheres with edge length $e = 1$ and height $h = c = \frac{1}{2}$. This gives for the nearest-neighbor distances in the A layer $a = \frac{3}{2}$, and therefore a ratio of $\gamma = c/a = \frac{2}{3}$. Such a lattice is best described by linear chains along the c axis with atoms from the A layers and shifted by c/a atoms from the C layers (notice that in the region $\gamma < \frac{2}{3}$ we have $\kappa = 2$). As the kissing number is $\kappa = 8$ at the boundary (see Fig. 2), we expect that the minimum occurs at higher energies compared to the one around $\gamma_{\text{hcp}} = \sqrt{\frac{8}{3}}$.

For very soft potentials (low values of m) the minimum disappears. This happens exactly at the point when the minimum becomes a turning point at the critical exponents of $(n_c, m_c), (n_c > m_c)$ where we have the conditions $\partial_\gamma E_{nm}^{*}(\gamma) = 0$ and $\partial_\gamma^2 E_{nm}^{*}(\gamma) = 0$. This is shown in Fig. 7. We derived the curve by searching numerically for the turning point close to $\gamma = 2/3$. When $m = n$, the cohesive energy is interpreted via its limit. Let

$$E_m^{*}(\gamma) = \lim_{n\to m} E_{nm}^{*}(\gamma). \tag{56}$$

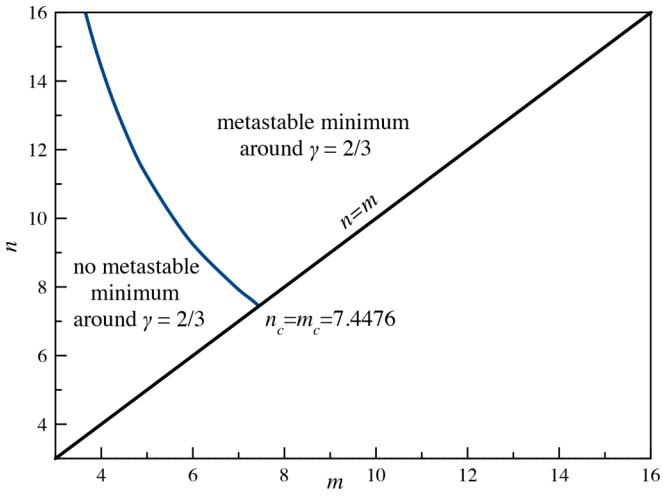

FIG. 7. Critical (n, m) values $((n_c, m_c), n_c > m_c)$ where the metastable minimum becomes a turning point.

Then from (55) we have

$$\log[-2E_m^{*}(\gamma)] = \lim_{n\to m} \log\left(\frac{L^{\text{hcp}}\left(\frac{m}{2},\gamma\right)^n}{L^{\text{hcp}}\left(\frac{n}{2},\gamma\right)^m}\right)^{\frac{1}{n-m}} = \lim_{n\to m} \frac{n\log L^{\text{hcp}}\left(\frac{m}{2},\gamma\right) - m\log L^{\text{hcp}}\left(\frac{n}{2},\gamma\right)}{n-m}. \tag{57}$$

By l'Hôpital's rule this becomes

$$\begin{aligned}\log[-2E_m^{*}(\gamma)] &= \lim_{n\to m} \frac{\partial}{\partial n}\left[n\log L^{\text{hcp}}\left(\frac{m}{2},\gamma\right) - m\log L^{\text{hcp}}\left(\frac{n}{2},\gamma\right)\right] \\ &= \log L\left(\frac{m}{2},\gamma\right) - \frac{mL'\left(\frac{m}{2},\gamma\right)}{2L\left(\frac{m}{2},\gamma\right)},\end{aligned} \tag{58}$$

where in the last line we have written $L(\frac{m}{2},\gamma)$ for $L^{\text{hcp}}(\frac{m}{2},\gamma)$, and the prime denotes differentiation with respect to the first variable:

$$L'(s,\gamma) = \frac{\partial}{\partial s} L^{\text{hcp}}(s,\gamma). \tag{59}$$

On exponentiating it follows that

$$E_m^{*}(\gamma) = \lim_{n\to m} E_{nm}^{*}(\gamma) = -\frac{1}{2}L\left(\frac{m}{2},\gamma\right)\exp\left[-\frac{mL'\left(\frac{m}{2},\gamma\right)}{2L\left(\frac{m}{2},\gamma\right)}\right]. \tag{60}$$

This function was used to numerically determine the bound $7.44760 < n_c = m_c < 7.44761$ which is depicted in Fig. 7 as $n_c = m_c = 7.4476$. For, when $n_c = m_c = 7.44761$, the function $E_m^{*}(\gamma)$ in (60) has a minimum at $\gamma = 0.77580$ followed closely by a maximum at $\gamma = 0.77598$. Between the minimum and maximum is an inflection point at $\gamma = 0.775887$

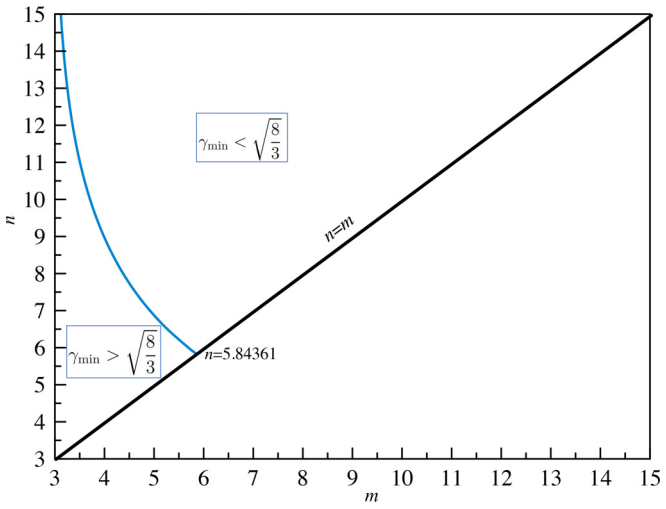

FIG. 8. Dividing (n, m) areas $(n > m)$ of regions where $\gamma_{\min} > \gamma_{\text{hcp}}$ and $\gamma_{\min} < \gamma_{\text{hcp}}$. Note that the dividing line intersects with the $n = m$ line at $n = 5.84361$ and approaches $m = 3$ for $n \to \infty$.

where we have

$$\left.\frac{\partial E^*_{m=7.44761}(\gamma)}{\partial \gamma}\right|_{\gamma=0.775887} = 1.373$$

$$\text{and} \quad \left.\frac{\partial^2 E^*_{m=7.44761}(\gamma)}{\partial \gamma^2}\right|_{\gamma=0.775887} = 0. \tag{61}$$

For smaller values of $n_c = m_c$ (e.g., by reducing the digit in the fifth decimal place by 1) the metastable minimum and maximum merge together and hence collapse, leaving just the inflection point. Thus, when $n_c = m_c = 7.44760$ we have

$$\left.\frac{\partial E^*_{m=7.44760}(\gamma)}{\partial \gamma}\right|_{\gamma=0.775887} = -9.137$$

$$\text{and} \quad \left.\frac{\partial^2 E^*_{m=7.44760}(\gamma)}{\partial \gamma^2}\right|_{\gamma=0.775887} = 0. \tag{62}$$

We also note the singularity at $m = 3$.

In regard to the global minimum, there is no reason for the LJ potential to have the minimum exactly at $\gamma_{\text{hcp}} = \sqrt{\frac{8}{3}}$ as the first derivatives $\partial_\gamma E^*_{nm}(\gamma_{\text{hcp}})$ in Table I show for various (n, m) combinations. Indeed, it was already shown by Howard [29] by direct lattice summations over 450 shells around a central atom that the minimum occurs at 99.986% of the ideal hcp value for the (12,6) LJ potential. To obtain more detailed information if $\gamma_{\min}$ is greater or lower than γ_{hcp} we used a Newton-Raphson procedure as described in Appendix C. The dividing line between the two regions of $\gamma < \sqrt{\frac{8}{3}}$ and $\gamma > \sqrt{\frac{8}{3}}$ is shown in Fig. 8. Only for very soft potentials (low n and m values) does the minimum come at values $\gamma_{\min} > \gamma_{\text{hcp}}$. For the common (12,6) LJ potential, $\gamma_{\min} = 1.6327633 < \gamma_{\text{hcp}}$. However, the deviations δ_{nm} defined by $\gamma_{\min} = \sqrt{\frac{8}{3}} + \delta_{nm}$ are very small, and so are the energy differences between the minimum and the ideal hcp structure; see Table III. To give a real example we take argon with a dissociation energy of $\epsilon = 1191$ J/mol for the dimer [30]. The change due to the deviation from the ideal c/a ratio is therefore $\Delta E_{nm} = \Delta E^*_{nm}\epsilon = -8.661 \times 10^{-4}$ J/mol. This value is far smaller than the accuracy which can be achieved in any solid-state calculation [31]. Accordingly, for the deviation $\delta_{nm} = 7.701 \times 10^{-4}$ we use the equilibrium distance of 3.3502 Å of Azis [30] and obtain a slight difference in the atomic distance between the pair of six neighboring atoms. Such a small deviation is perhaps within experimental reach.

When considering the hard-sphere limit with an attractive a^{-n} potential in (64), we present the (100,6) LJ potential ($s = 50$ and 3, respectively, in our earlier definition) in Fig. 8 as best candidate, as it is still numerically manageable despite the large exponent of $m = 100$. Here the deviation δ_{nm} listed in Fig. 8 is indeed very small. The curve shows a rather peculiar behavior around $\gamma = \sqrt{\frac{8}{3}}$ going steeply towards infinity for $\gamma_{\text{hcp}} \leqslant \sqrt{\frac{8}{3}}$. For an infinite repulsive wall the minimum sits at exactly $\gamma_{\text{hcp}} = \sqrt{\frac{8}{3}}$ as one expects. For values of $\gamma < \sqrt{\frac{8}{3}}$ and $m < \infty$ we enter a steep repulsive wall where the atoms in the hexagonal closed packed sheets need to give space for the next layer.

B. The (a, c) parameter space

Here we include the derivatives of the lattice sum expressions with respect to a. Using reduced units for a, c, and E in (64) and omitting the asterisk in our notation (or setting $r_e = 1$ and $\epsilon = 1$) we have

$$E^{\text{coh}}_{\text{LJ}}(n, m, a, c) = \frac{nm}{2(n-m)}\left[\frac{L^{\text{hcp}}\left(\frac{n}{2}, \frac{c}{a}\right)}{n}a^{-n} - \frac{L^{\text{hcp}}\left(\frac{m}{2}, \frac{c}{a}\right)}{m}a^{-m}\right]. \tag{63}$$

At fixed c value we need the minimum of the cohesive energy with respect to a, $\partial E^{\text{coh}}_{\text{LJ}}(n, m, a, c)/\partial a$. This leads to the

TABLE III. $\partial_\gamma E^*_{nm}(\gamma_{\text{hcp}})$, $\delta_{nm} = \gamma_{\min} - \sqrt{\frac{8}{3}}$, and $\Delta E^*_{nm} = E^*_{nm}(\gamma_{\min}) - E^*_{nm}(\gamma_{\text{hcp}})$ for various (n, m) LJ potentials. Note that the exponents n, m are multiplied by 2 compared to the s exponent used in the previous sections.

n	m	$E^*_{nm}(\gamma_{\min})$	δ_{nm}	ΔE^*_{nm}	$\partial_\gamma E^*_{nm}(\gamma_{\text{hcp}})$
12	6	−8.611070	-2.298569×10^{-4}	-7.272348×10^{-7}	6.327613×10^{-3}
6	4	−38.932531	3.077860×10^{-4}	-2.121345×10^{-6}	-1.378463×10^{-2}
12	4	−18.309854	-8.758790×10^{-5}	-1.526585×10^{-7}	3.485817×10^{-3}
20	6	−7.825827	-1.404378×10^{-4}	-3.993197×10^{-7}	5.686712×10^{-3}
20	12	−6.161877	-6.980408×10^{-5}	-1.518888×10^{-7}	4.351831×10^{-3}
100	6	−7.313826	-2.186397×10^{-5}	-2.082085×10^{-7}	4.013898×10^{-3}

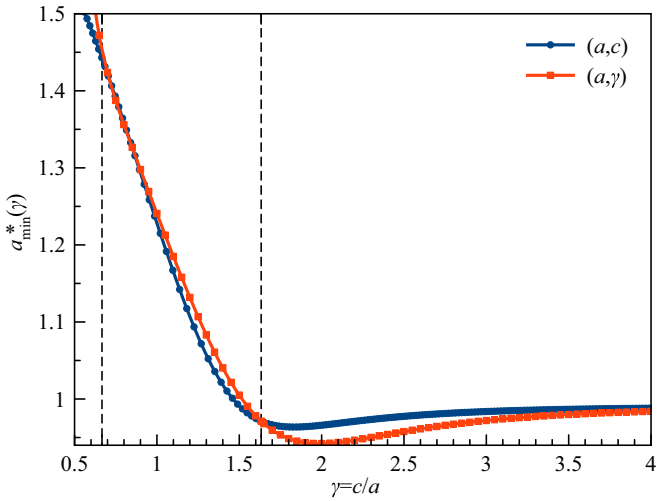

FIG. 9. The lattice parameter $a^*_{\min}(\gamma)$ for the (12,6) LJ potential. Results from both parameter spaces (a, γ) and (a, c) are shown.

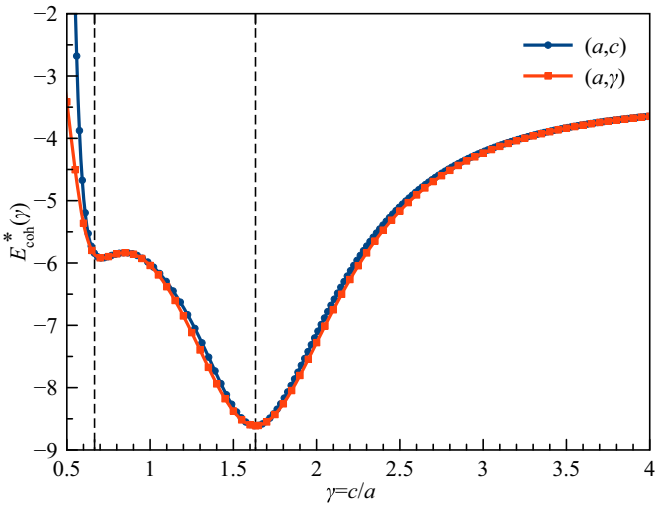

FIG. 10. The cohesive energy $E^*_{\rm coh}(\gamma)$ for the (12,6) LJ potential. Results from both parameter spaces (a, γ) and (a, c) are shown.

condition

$$nma^m L^{\rm hcp}\left(\frac{n}{2}, \frac{c}{a}\right) - nma^n L^{\rm hcp}\left(\frac{m}{2}, \frac{c}{a}\right) - ma^{m+1}\frac{\partial L^{\rm hcp}\left(\frac{n}{2}, \frac{c}{a}\right)}{\partial a} + na^{n+1}\frac{\partial L^{\rm hcp}\left(\frac{m}{2}, \frac{c}{a}\right)}{\partial a} = 0. \quad (64)$$

This again requires derivatives of Bessel functions and we get a more complicated expression compared to (54). The first and second derivatives required for the Newton-Raphson method to determine $a_{\min}$ at fixed c are given in Appendix D.

Figure 9 shows the dependence of the lattice parameter $a_{\min}$ with respect to γ which minimizes the cohesive energy for the (12,6) LJ potential. A comparison with the corresponding curve in Fig. 4 shows a clear difference between the two optimized lattice parameters a for the two different parameter sets used. However, we get a very similar picture for the cohesive energies as shown in Fig. 10, which justifies the approximation used in the previous section. Moreover, the metastable minimum around $\gamma = 2/3$ is apparent in both curves.

V. ANALYTIC CONTINUATION OF THE LATTICE SUM $L^{\rm hcp}(s)$

We show that the lattice sum $L^{\rm hcp}(s)$ can be continued analytically to the whole s plane and that the resulting functions have a single simple pole at $s = 3/2$ and no other singularities. We start by determining the residue of $L^{\rm hcp}(s)$ at $s = 3/2$. In the formula (50), all of the terms are analytic at $s = 3/2$ except for the term involving $\zeta(2s-2)$, which has a simple pole there. Therefore, the Laurent series for $L^{\rm hcp}(\gamma, s)$ around the pole at $s = 3/2$ is of the form

$$L^{\rm hcp}(s, \gamma) = \frac{d_{-1}}{s - 3/2} + d_0 + \sum_{n\in\mathbb{N}} d_n (s - 3/2)^n, \quad (65)$$

where

$$d_{-1} = \mathrm{Res}(L^{\rm hcp}(s), 3/2) = \frac{8\pi}{\gamma\sqrt{3}} \quad (66)$$

and

$$d_0(\gamma) = 6\zeta(3/2)L_{-3}(3/2) + \frac{16\pi}{\gamma\sqrt{3}}[\gamma_0 + \ln(2/\gamma) - 1] + \frac{4}{\sqrt{3}}\frac{(2\pi)^{3/2}}{\Gamma(3/2)}\sum_{k\in\mathbb{N}}\sum_{N\in\mathbb{N}} u_2(N)\left(\frac{N}{3\gamma^2k^2}\right)^{1/4} K_{1/2}\left(\frac{4\pi}{\sqrt{3}}\gamma k\sqrt{N}\right)$$
$$+ \frac{4}{\sqrt{3}}\frac{(2\pi)^{3/2}}{\Gamma(3/2)}\sum_{k\in\mathbb{N}_0}\sum_{N\in\mathbb{N}} \cos\left(\frac{2\pi N}{3}\right) u_2(N)\left(\frac{N}{3\gamma^2\left(k+\frac{1}{2}\right)^2}\right)^{1/4} K_{1/2}\left(\frac{4\pi}{\sqrt{3}}\gamma\left(k+\frac{1}{2}\right)\sqrt{N}\right). \quad (67)$$

$\gamma_0 = 0.57721566490153286\ldots$ is the Euler-Mascheroni constant. The derivation of the residue and the second term in Eq. (67) is given in Appendix B. Using well-known relations for the Bessel function $K_{1/2}(x) = \sqrt{\pi/2x}\, e^{-x}$ we obtain

$$d_0(\gamma) = 6\zeta(3/2)L_{-3}(3/2) + \frac{16\pi}{\gamma\sqrt{3}}[\gamma_0 + \ln(2/\gamma) - 1] + \frac{8\pi}{\gamma\sqrt{3}}\sum_{k\in\mathbb{N}}\sum_{N\in\mathbb{N}}\frac{1}{k}u_2(N)\exp\left(-\frac{4\pi}{\sqrt{3}}\gamma k\sqrt{N}\right)$$
$$+ \frac{8\pi}{\gamma\sqrt{3}}\sum_{k\in\mathbb{N}_0}\sum_{N\in\mathbb{N}}\frac{\cos\left(\frac{2\pi N}{3}\right)}{\left(k+\frac{1}{2}\right)}u_2(N)\exp\left(-\frac{4\pi}{\sqrt{3}}\gamma\left(k+\frac{1}{2}\right)\sqrt{N}\right)$$

$$= 6\zeta(3/2)\,L_{-3}(3/2) \;+\; \frac{16\pi}{\gamma\sqrt{3}}\,[\gamma_0 + \ln(2/\gamma) - 1] - \frac{8\pi}{\gamma\sqrt{3}}\sum_{N=1}^{\infty} u_2(N)\ln(1 - e^{-\frac{4\pi}{\sqrt{3}}\gamma k\sqrt{N}})$$

$$+ \frac{8\pi}{\gamma\sqrt{3}}\sum_{N\in\mathbb{N}} \cos\left(\frac{2\pi N}{3}\right) u_2(N)\,\ln\left(\frac{1 + e^{-\frac{2\pi}{\sqrt{3}}\gamma k\sqrt{N}}}{1 - e^{-\frac{2\pi}{\sqrt{3}}\gamma k\sqrt{N}}}\right). \tag{68}$$

Here we use the series expansion for the logarithm

$$\ln(1+x) = \sum_{k\in\mathbb{N}} \frac{(-1)^{k+1}}{k} x^k \quad \text{or} \quad \ln(1-x) = -\sum_{k\in\mathbb{N}} \frac{1}{k} x^k, \tag{69}$$

substituting $x \to e^{-x}$. For the special value of $\gamma_{\text{hcp}} = \sqrt{8/3}$ we have

$$d_0(\sqrt{8/3}) = 6.984623741438416613 07\ldots. \tag{70}$$

Concerning the analytical continuation to the left of the simple pole, $s < 3/2$, by (A6) the double series of Bessel functions in (50) converges absolutely and uniformly on compact subsets of the s plane and therefore represents an entire function of s. It follows that L^{hcp} has an analytic continuation to a meromorphic function. Moreover, the Laurent expansion (65) converges for all $s \neq 3/2$. Further inspection reveals that the only problematic case in (50) is for $s = 1$ because of the two terms having canceling singularities. Therefore we take $s = 1$ in the second formula (51) instead to obtain

$$L^{\text{hcp}}(1) = \frac{\pi^2}{3\gamma^2} + \frac{3\pi}{\gamma}\,(\sqrt{3}+1)\,\zeta(1/2)\,L_{-3}(1/2) + \frac{2\pi}{\gamma}\sum_{N\in\mathbb{N}} \frac{u_2(N)}{\sqrt{N}}\left[\exp\left(\frac{2\pi\sqrt{N}}{\gamma}\right) - 1\right]^{-1}$$

$$- \frac{\pi}{\gamma}\sum_{N\in\mathbb{N}_0} \frac{u_2(3N+1)}{\sqrt{N+\frac{1}{3}}}\left[\exp\left(\frac{2\pi\sqrt{N+\frac{1}{3}}}{\gamma}\right) - 1\right]^{-1}, \tag{71}$$

where we have used (A5) for the modified Bessel function of the second kind, and used the geometric series to evaluated the sum over k. For the special value of $\gamma_{\text{hcp}} = \sqrt{8/3}$ we have

$$L^{\text{hcp}}(1, \gamma = \sqrt{8/3}) = -11.432653001495285 63572\ldots. \tag{72}$$

We also record the result

$$L^{\text{hcp}}(1/2) = 6\zeta(1/2)L_{-3}(1/2) + \frac{\pi\gamma}{3\sqrt{3}} + 2\sum_{N\in\mathbb{N}} \frac{u_2(N)}{\sqrt{N}}\left[\exp\left(\frac{4\pi}{\sqrt{3}}\gamma\sqrt{N}\right) - 1\right]^{-1}$$

$$+ 2\sum_{N\in\mathbb{N}} \cos\left(\frac{2\pi N}{3}\right)\frac{u_2(N)}{\sqrt{N}}\left[\exp\left(\frac{2\pi}{\sqrt{3}}\gamma\sqrt{N}\right) - \exp\left(-\frac{2\pi}{\sqrt{3}}\gamma\sqrt{N}\right)\right]^{-1},$$

which is obtained in the same way, starting from (50) and using the symmetry for the Bessel function, $K_{-s}(x) = K_s(x)$. We obtain using $\gamma = \sqrt{8/3}$,

$$L^{\text{hcp}}(1/2, \gamma = \sqrt{8/3}) = -3.241858615075732 86473\ldots. \tag{73}$$

Finally, using (51) we observe that $L^{\text{hcp}}(0) = 2\zeta(0) = -1$ for all $\gamma > 0$.

A graph of the function $L^{\text{hcp}}(s)$ is shown in Fig. 11 for the case $\gamma_{\text{hcp}} = \sqrt{8/3}$. We see that the curve has zeros at $s = -1, -2, -3, \ldots$ as we have $\Gamma(s) \to \infty$ for $s \in -\mathbb{N}_0$, and the Bessel terms vanish in both Eqs. (50) and (51). Taking (51), the only remaining term for $n \in \mathbb{N}$ is $2\gamma^{-2s}\zeta(2s)$, and $\zeta(s)$ has zeros exactly at $s = -2, -4, -6, \ldots$.

VI. CAN ANALYTICAL CONTINUATION BE USED FOR THE KRATZER POTENTIAL?

It is well known that for the Madelung constant analytical continuation can be used where the underlying series is only conditionally convergent [32]. The (2,1) LJ potential is known as the Kratzer potential. Introduced in 1920 for vibrational levels in diatomic molecules,[33] it has the form

$$V_{\text{Kratzer}}(r)/\epsilon = \left[\left(\frac{r_e}{r}\right)^2 - 2\left(\frac{r_e}{r}\right)\right] \tag{74}$$

and is analogous to the LJ potential shown in (1) with $n = 2$ and $m = 1$. The Kratzer potential has a Coulomb-like behavior in the long range and a harmonic repulsive behavior in the short range. It is a very soft potential compared to the usual (12,6) LJ potential and could in principle be useful for example for metallic interaction. The question arises if we can use Eq. (2), which requires lattice sums to the left of the singularity at $s = \frac{3}{2}$ where $L_3^{\text{hcp}}(s = 1) < 0$ for $s \in (0, \frac{3}{2})$. It is sufficient to consider the ideal hcp lattice only ($\gamma_{\text{hcp}} = \sqrt{8/3}$).

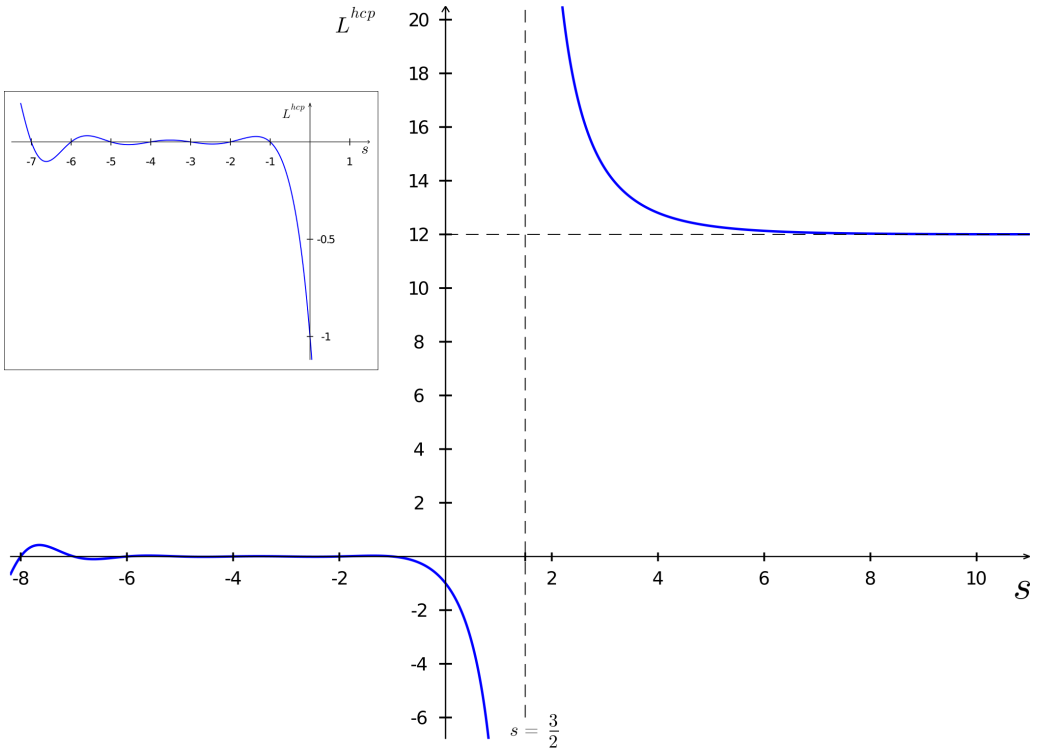

FIG. 11. Graph of $L^{\mathrm{hcp}}(s)$ for $-10 < s < 10$ (inlet shows the region $-7 < s < 0$).

By taking $n = 2$ and $m = 1$ in (64), the Kratzer potential dependent on the lattice constant a then becomes

$$E^{\mathrm{coh}}_{\mathrm{Kratzer}}(a,\gamma)/\epsilon = \frac{r_e^2}{2a^2}L^{\mathrm{hcp}}(1,\gamma) - \frac{r_e}{a}L^{\mathrm{hcp}}\left(\frac{1}{2},\gamma\right), \quad (75)$$

for which the required lattice sums are given in Eqs. (50) and (51).

The Kratzer potential together with the cohesive energy is shown in Fig. 12. The cohesive energy has a maximum and

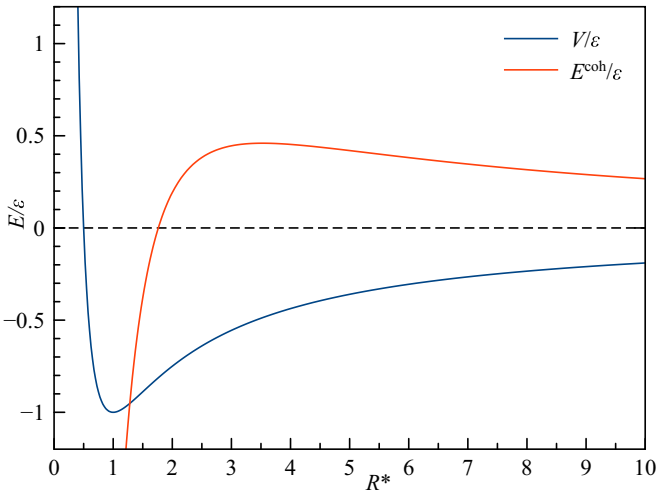

FIG. 12. Kratzer potential for $V_{\mathrm{Kratzer}}(R^*)/\epsilon$ with $R^* = r/r_e$ and for the cohesive energy $E^{\mathrm{coh}}_{\mathrm{Kratzer}}(R^*)/\epsilon$ with $R^* = a/r_e$ where a is the hcp lattice constant and $c/a = \gamma = \sqrt{8/3}$.

not a minimum as it should. The distance and energy can be obtained from (54) and (55):

$$a^*_{\mathrm{min}} = \frac{L\left(1,\sqrt{\frac{8}{3}}\right)}{L\left(\frac{1}{2},\sqrt{\frac{8}{3}}\right)} = \frac{-11.432653001495}{-3.241858615076} = 3.526573598346, \quad (76)$$

$$E^*(a^*_{\mathrm{min}}) = E^{\mathrm{coh}}_{\mathrm{Kratzer}}(a^*_{\mathrm{min}})/\epsilon = -\frac{L\left(\frac{1}{2},\sqrt{\frac{8}{3}}\right)^2}{2L\left(1,\sqrt{\frac{8}{3}}\right)} = +0.459632916295. \quad (77)$$

Even if only positive lattice sums are taken to obtain a proper cohesive energy curve with a minimum instead of a maximum, the nearest-neighbor distance increases from the dimer to the solid state contrary to the (12,6) LJ potential. This clearly demonstrates that the Kratzer potential gives nonphysical results for the hcp lattice as the exponents lie left to the pole at $s = \frac{3}{2}$ producing negative lattice sums in the required region. Even if absolute values of $L^{\mathrm{hcp}}(s)$ are used instead to invert the shape and produce a minimum, it would lack physical justification. The situation does not change if we choose $n < 3$ and $m > 3$ for a (n, m) LJ potential. As there is no alternative to an analytic continuation, the Kratzer potential cannot be used for the hcp lattice Moreover, this result does not change for any Bravais lattice with its associated positive definite Gram matrix as the underlying Epstein zeta function for lattice sums converges absolutely only for $s > N/2$ [34], where N is the dimension of the lattice. This is in stark contrast to the Madelung constant described by an alternating

series. The main difference here is that the Madelung constant is a smooth function over the whole range of real exponents containing no singularities [14,35].

VII. RELATION BETWEEN THE HCP STRUCTURE AND THE CUBOIDAL LATTICES

We recently introduced lattice sums for cubic lattices by introducing the following basis vectors [15]:

$$\boldsymbol{b}_1^\top(A) = (1,0,0), \quad \boldsymbol{b}_2^\top(A) = \left(\frac{A}{A+1}, \frac{\sqrt{2A+1}}{A+1}, 0\right),$$
$$\boldsymbol{b}_3^\top(A) = \left(\frac{1}{A+1}, \frac{1}{(A+1)\sqrt{2A+1}}, \sqrt{\frac{4A}{(A+1)(2A+1)}}\right), \tag{78}$$

where $A = 1/2$ defines the body-centered cubic (bcc) lattice and $A = 1$ the face-centered cubic (fcc) lattice. The packing density has been obtained as [15]

$$\rho(A) = \frac{\pi}{12}\sqrt{\frac{(A+1)^3}{A}}. \tag{79}$$

We can compare this to the hcp lattice with $\gamma \geqslant \sqrt{8/3}$ derived from the volume (10),

$$\rho(\gamma) = \frac{2\pi}{3\gamma\sqrt{3}}. \tag{80}$$

As the validity range for hard-sphere packing is $\gamma \in [\sqrt{8/3}, \infty)$ we see that the largest packing density is achieved by the ideal value of $\gamma = \sqrt{8/3}$. Comparing both densities, hcp has the same packing density as the cuboidal lattices for

$$\gamma = \sqrt{\frac{8}{3}}\, f(A) \quad \text{with} \quad f(A) = \sqrt{\frac{8A}{(A+1)^3}}. \tag{81}$$

Again, for $A = 1$ (fcc) we see that the packing density is identical to the ideal hcp structure. For $A = 1/2$ (bcc) $f(A) = 1.08866\ldots$, that is, the hcp structure has the same packing density compared to bcc if we increase the c/a ratio by approximately 8.9%.

The corresponding lattice sum for the cuboidal lattice was already given in Ref. [15]:

$$L^{\text{cub}}(s,A) = 4\left(\frac{A+1}{2}\right)^s \zeta(s) L_{-4}(s) + \frac{\pi A}{s-1}\left(1+\frac{1}{A}\right)^s \zeta(2s-2) + \frac{2\pi^s\sqrt{A}}{\Gamma(s)}\left(\sqrt{A}+\frac{1}{\sqrt{A}}\right)^s \sum_{i=1}^{\infty}\sum_{N=1}^{\infty} r_2(N)\left(\frac{N}{i^2}\right)^{(s-1)/2}$$
$$\times K_{s-1}(2\pi i\sqrt{AN}) + \frac{2\pi^s\sqrt{A}}{\Gamma(s)}\left(\sqrt{A}+\frac{1}{\sqrt{A}}\right)^s \sum_{i=1}^{\infty}\sum_{N=0}^{\infty}(-1)^i r_2(4N+1)\left(\frac{2N+\frac{1}{2}}{i^2}\right)^{(s-1)/2} K_{s-1}\left(2\pi i\sqrt{A\left(2N+\frac{1}{2}\right)}\right), \tag{82}$$

where the L_{-4} function is defined in Appendix A. $L^{\text{cub}}(A;s)$ has a simple pole at $s = 3/2$, and the residue is given by

$$\text{Res}(L^{\text{cub}}(A;s), 3/2) = \frac{\pi}{\sqrt{A}}(A+1)^{3/2}. \tag{83}$$

It follows that the difference between the two lattice sums, cuboidal and hcp, the singularity is removed if

$$\text{Res}(L^{\text{cub}}(s,A), 3/2) - \text{Res}(L^{\text{hcp}}(s,\gamma), 3/2) = d_{-1}^{\text{cub}} - d_{-1}^{\text{hcp}}$$
$$= \frac{\pi}{\sqrt{A}}(A+1)^{3/2} - \frac{8\pi}{\gamma\sqrt{3}} = 0. \tag{84}$$

This gives the condition in (81). Hence we follow that the singularity at $s = 3/2$ is removed for the difference between the cuboidal lattices and the hcp structure if they have the same packing density. Notice, that in removing the singularity we do not just have to consider hard spheres and only need the condition in (81) that $\gamma > 0$.

Evaluating the coefficient for d_0^{cub} given in Ref. [15] and using (70) we obtain

$$\lim_{s\to\frac{3}{2}}\{L^{\text{cub}}(s,A=1) - L^{\text{hcp}}(s,\gamma=\sqrt{8/3})\}$$
$$= -0.00057119111616867901\ldots. \tag{85}$$

The difference $L^{\text{hcp}}(s,\gamma=\sqrt{8/3}) - L^{\text{cub}}(s,A=1)$ is shown in Fig. 13. What is evident is that the difference in lattice sums between fcc and hcp is very small which is reflected in the fact that both phases often coexist for real compounds. The graph also appears to suggest the following for the relation between

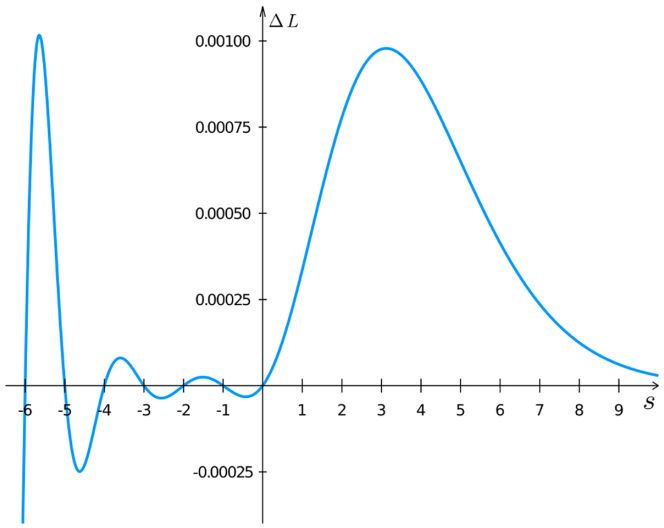

FIG. 13. Graph of $L^{\text{hcp}}(s) - L^{\text{fcc}}(s)$.

the ideal hcp and fcc structures:

$$L^{\rm hcp}(s) > L^{\rm fcc}(s) > 0 \quad \text{for} \quad s \in \cdots \cup (-6,-5) \cup (-4,-3) \cup (-2,-1) \cup (3/2,\infty),$$
$$L^{\rm hcp}(s) < L^{\rm fcc}(s) < 0 \quad \text{for} \quad s \in \cdots \cup (-5,-4) \cup (-3,-2) \cup (-1,0),$$
$$-1 > L^{\rm hcp}(s) > L^{\rm fcc}(s) \quad \text{for} \quad s \in (0,3/2).$$

VIII. CONCLUSIONS

We presented an efficient and fast convergent expansion for the multilattice hcp with variable c/a ratio. We demonstrated that the series can be analytically continued, albeit while mathematically sound the physical relevance has to be questioned at least for LJ type of potentials. We also showed that a metastable minimum appears for the (12,6) LJ potential at $\gamma = 0.71$, close to $\gamma = \frac{2}{3}$ where the kissing number is $\kappa = 8$, and showed its dependence on the choice of exponents n and m. For the minimum close to the ideal c/a ratio of $\gamma_{\rm hcp} = \sqrt{\frac{8}{3}}$ we discussed the slight symmetry breaking for $(n.m)$ LJ potentials where the sign of $\delta_{nm} = \gamma_{\rm min} - \sqrt{\frac{8}{3}}$ depends on the parameter range (n, m). It is clear that out results will be dependent upon changing the pressure and temperature [36,37], which is currently under investigation. As a final remark, we mention that many-body forces in real bulk systems can stabilize the minimum around $\gamma = \frac{2}{3}$ as this is well known, for example, for metallic systems [38]. The program for calculating lattice sums is freely available from our website [39].

APPENDIX A: FORMULAS FOR SPECIAL FUNCTIONS

Many results for special functions and analytic number theory have been used in this work. For clarity and ease of use, they are stated here along with references if not given in the books by Andrews *et al.* [40] or Temme [41].

1. The gamma function

The gamma function may be defined for $s > 0$ by

$$\Gamma(s) = \int_{[0,\infty)} t^{s-1}\, e^{-t}\, dt. \tag{A1}$$

By the change of variable $t = wx$ this can be rewritten in the useful form

$$\frac{1}{w^s} = \frac{1}{\Gamma(s)} \int_{[0,\infty)} x^{s-1}\, e^{-wx}\, dx. \tag{A2}$$

2. The modified Bessel function

The following integral may be evaluated in terms of the modified Bessel function:

$$\int_{[0,\infty)} x^{s-1} e^{-ax-b/x} dx = 2\left(\frac{b}{a}\right)^{s/2} K_s(2\sqrt{ab}). \tag{A3}$$

By the change of variable $x = u^{-1}$ it can be shown that

$$K_s(z) = K_{-s}(z). \tag{A4}$$

When $s = 1/2$ the modified Bessel function reduces to an elementary function:

$$K_{1/2}(z) = \sqrt{\frac{\pi}{2z}}\, e^{-z}. \tag{A5}$$

The asymptotic formula holds:

$$K_s(z) \sim \sqrt{\frac{\pi}{2z}}\, e^{-z} \quad \text{as} \quad z \to \infty, \quad (|\arg z| < 3\pi/2). \tag{A6}$$

3. Theta functions

The transformation formula for theta functions is [40,42]

$$\sum_{n\in\mathbb{Z}} e^{-\pi n^2 t + 2\pi i n a} = \frac{1}{\sqrt{t}} \sum_{n\in\mathbb{Z}} e^{-\pi (n+a)^2/t}, \quad \text{assuming } \mathrm{Re}(t) > 0. \tag{A7}$$

We will need the special cases $a = 0$ and $a = 1/2$, which are

$$\sum_{n\in\mathbb{Z}} e^{-\pi n^2 t} = \frac{1}{\sqrt{t}} \sum_{n\in\mathbb{Z}} e^{-\pi n^2/t} \tag{A8}$$

and

$$\sum_{n\in\mathbb{Z}} (-1)^n e^{-\pi n^2 t} = \frac{1}{\sqrt{t}} \sum_{n\in\mathbb{Z}} e^{-\pi (n+\frac{1}{2})^2/t}, \tag{A9}$$

respectively. The sum of two squares formula is [43]

$$\left(\sum_{j\in\mathbb{Z}} q^{j^2}\right)^2 = \sum_{j,k\in\mathbb{Z}} q^{j^2+k^2} = \sum_{N\in\mathbb{N}_0} r_2(N) q^N, \tag{A10}$$

where

$$r_2(N) = \#\{j^2 + k^2 = N\} = \begin{cases} 1 & \text{if } N = 0, \\ 4\sum_{d|N} \chi_{-4}(d) & \text{if } N \geqslant 1, \end{cases} \tag{A11}$$

$\chi_{-4}(d) = \sin(\pi d/2)$ and the sum is over the positive divisors d of N. For example,

$$\begin{aligned} r_2(18) &= 4[\chi_{-4}(1) + \chi_{-4}(2) + \chi_{-4}(3) \\ &\quad + \chi_{-4}(6) + \chi_{-4}(9) + \chi_{-4}(18)] \\ &= 4(1 + 0 - 1 + 0 + 1 + 0) = 4. \end{aligned}$$

The cubic analogs of the transformation formula are [42,44]

$$\sum_{j,k\in\mathbb{Z}} e^{-2\pi (j^2+jk+k^2)t} = \frac{1}{t\sqrt{3}} \sum_{j,k\in\mathbb{Z}} e^{-2\pi (j^2+jk+k^2)/3t} \tag{A12}$$

and

$$\sum_{j,k\in\mathbb{Z}} e^{-2\pi[(j+\frac{1}{3})^2+(j+\frac{1}{3})(k+\frac{1}{3})+(k+\frac{1}{3})^2]t} = \frac{1}{t\sqrt{3}} \sum_{j,k\in\mathbb{Z}} \omega^{j-k} e^{-2\pi(j^2+jk+k^2)/3t}, \tag{A13}$$

where $\omega = \exp(2\pi\sqrt{-1}/3)$ is a primitive cube root of unity. The analog of the sum of two squares result is [43]

$$\sum_{j,k\in\mathbb{Z}} q^{j^2+jk+k^2} = \sum_{N\in\mathbb{N}_0} u_2(N) q^N, \tag{A14}$$

where

$$u_2(N) = \#\{j^2+jk+k^2 = N\} = \begin{cases} 1 & \text{if } N=0, \\ 6\sum_{d|N} \chi_{-3}(d) & \text{if } N \geqslant 1, \end{cases} \tag{A15}$$

$$\text{with } \chi_{-3}(d) = \frac{\sin(2\pi d/3)}{\sin(2\pi/3)}$$

and the sum is again over the positive divisors d of N. By Ref. [43] we also have

$$\sum_{j,k\in\mathbb{Z}} q^{(j+\frac{1}{3})^2+(j+\frac{1}{3})(k+\frac{1}{3})+(k+\frac{1}{3})^2} = \frac{1}{2} \sum_{N\in\mathbb{N}_0} u_2(3N+1) q^{N+\frac{1}{3}}. \tag{A16}$$

4. The Riemann zeta function and *L* functions

The definitions are

$$\zeta(s) = \sum_{j\in\mathbb{N}} \frac{1}{j^s}, \tag{A17}$$

$$L_{-3}(s) = \sum_{j\in\mathbb{N}} \frac{\chi_{-3}(j)}{j^s} = 1 - \frac{1}{2^s} + \frac{1}{4^s} - \frac{1}{5^s} + \frac{1}{7^s} - \frac{1}{8^s} + \cdots.$$

$$L_{-4}(s) = \sum_{n\in\mathbb{N}} n^{-s} \sin\left(\frac{n\pi}{2}\right) = 4^{-s}\left[\zeta\left(s, \frac{1}{4}\right) - \zeta\left(s, \frac{3}{4}\right)\right] \tag{A18}$$

The function $\zeta(s)$ is the Riemann zeta function. It has a pole of order 1 at $s=1$, and in fact [40,41]

$$\lim_{s\to 1}(s-1)\zeta(s) = 1. \tag{A19}$$

We will require the functional equations

$$\pi^{-s/2}\Gamma(s/2)\zeta(s) = \pi^{-(1-s)/2}\Gamma((1-s)/2)\zeta(1-s) \tag{A20}$$

and the special values

$$\zeta(2) = \frac{\pi^2}{6}, \quad \zeta(0) = -\frac{1}{2}, \quad \zeta(-1) = -\frac{1}{12}, \quad \zeta(-2n) = 0 \quad \text{for} \quad n \in \mathbb{N} \tag{A21}$$

and

$$L_{-3}(1) = \frac{\pi\sqrt{3}}{9}, \quad L_{-3}(0) = \frac{1}{3}, \quad L_{-3}(-2n+1) = 0 \quad \text{for} \quad n \in \mathbb{N}. \tag{A22}$$

For details see Refs. [26,45]. Other results used are

$$\sum_{j\in\mathbb{N}_0} \frac{1}{(j+\frac{1}{2})^s} = (2^s-1)\zeta(s), \tag{A23}$$

$$\sum_{i,j\in\mathbb{Z}}{}' \frac{1}{(i^2+ij+j^2)^s} = 6\zeta(s)L_{-3}(s), \tag{A24}$$

$$\sum_{i,j\in\mathbb{Z}} \frac{1}{\left[\left(i+\frac{1}{3}\right)^2 + \left(i+\frac{1}{3}\right)\left(j+\frac{1}{3}\right) + \left(j+\frac{1}{3}\right)^2\right]^s} = 3(3^s-1)\zeta(s)L_{-3}(s). \tag{A25}$$

The identity (A23) follows from the definition of $\zeta(s)$ by series rearrangements. For (A24), see (1.4.16) of Ref. [12]. The identity (A25) can be obtained by the method of Mellin transforms [12,40,43].

APPENDIX B: LAURENT EXPANSION

Laurent's theorem implies there is an expansion of the form

$$L^{\text{hcp}}(s,\gamma) = \frac{d_{-1}}{s-3/2} + d_0 + \sum_{n=1}^{\infty} d_n (s-3/2)^n, \tag{B1}$$

where we get for (50) the residue (66). This follows from

$$\begin{aligned} &\lim_{s\to 3/2}(s-3/2)L^{\text{hcp}}(s) \\ &= \lim_{s\to 3/2}(s-3/2)\frac{4\pi}{\sqrt{3}(s-1)}\left(\frac{\gamma}{2}\right)^{2-2s}\zeta(2s-2) \\ &= \frac{16\pi}{\gamma\sqrt{3}} \lim_{s\to 3/2}(s-3/2)\zeta(2s-2) \\ &= \frac{8\pi}{\gamma\sqrt{3}} \lim_{u\to 1}(u-1)\zeta(u) = \frac{8\pi}{\gamma\sqrt{3}}, \end{aligned} \tag{B2}$$

where (A19) was used in the last step of the calculation. To get the coefficient d_0 in (50) we need to consider the following limit:

$$w = \lim_{s\to 3/2}\left[\frac{4\pi}{\sqrt{3}(s-1)}\left(\frac{\gamma}{2}\right)^{2-2s}\zeta(2s-1) - \frac{8\pi}{\gamma\sqrt{3}\left(s-\frac{3}{2}\right)}\right]. \tag{B3}$$

Substituting $s = (t+3)/2$ and using the Laurent expansion for the Riemann zeta function,

$$w = \lim_{t\to 0}\left\{\frac{8\pi}{\sqrt{3}(t+1)}\left(\frac{2}{\gamma}\right)^{t+1}[t^{-1}+\gamma_0-\gamma_1 t+\cdots]-\frac{16\pi}{\gamma t\sqrt{3}}\right\} \tag{B4}$$

$$= \lim_{t\to 0}\frac{f(t)-f(0)}{t} + \frac{16\pi}{\gamma\sqrt{3}}\gamma_0 = f'(t)|_0 + \frac{16\pi}{\gamma\sqrt{3}}\gamma_0,$$

where

$$f(t) = \frac{8\pi}{\sqrt{3}}\frac{1}{(t+1)}\left(\frac{2}{\gamma}\right)^{t+1} \tag{B5}$$

and $\gamma_0 = 0.57721566490153286060\ldots$ is Euler's constant. It is easy to verify that

$$f'(t) = -\frac{8\pi}{\sqrt{3}(t+1)^2}\left(\frac{2}{\gamma}\right)^{t+1} + \frac{8\pi}{\sqrt{3}(t+1)}\left(\frac{2}{\gamma}\right)^{t+1}\ln\left(\frac{2}{\gamma}\right). \tag{B6}$$

We finally obtain

$$w = \frac{16\pi}{\gamma\sqrt{3}}\left[\gamma_0+\ln\left(\frac{2}{\gamma}\right)-1\right]. \tag{B7}$$

APPENDIX C: MINIMUM OF LENNARD-JONES POTENTIALS NEAR $\gamma = \sqrt{\frac{8}{3}}$

The iterative Newton-Raphson algorithm [46] can be used to determine $\gamma_{\min}$ to the required accuracy

$$\gamma_{i+1} = \gamma_i - \frac{\partial_\gamma E^*_{nm}(\gamma_i)}{\partial^2_\gamma E^*_{nm}(\gamma_i)}, \tag{C1}$$

starting with $\gamma_1 = \sqrt{\frac{8}{3}}$. Only a few iterations are required to achieve convergence to computer accuracy. The required derivatives for $E^*_{nm}(\gamma)$ can be easily derived:

$$\partial_\gamma E^*_{nm}(\gamma) = \frac{1}{2(n-m)}\left[m\left(\frac{L(\frac{m}{2},\gamma)}{L(\frac{n}{2},\gamma)}\right)^{\frac{n}{n-m}}\partial_\gamma L\left(\frac{n}{2},\gamma\right) - n\left(\frac{L(\frac{m}{2},\gamma)}{L(\frac{n}{2},\gamma)}\right)^{\frac{m}{n-m}}\partial_\gamma L\left(\frac{m}{2},\gamma\right)\right],$$

$$\begin{aligned}\partial^2_\gamma E^*_{nm}(\gamma) = {}& \frac{nm}{2(n-m)^2}\left[L\left(\frac{n}{2},\gamma\right)\partial_\gamma L\left(\frac{m}{2},\gamma\right)+L\left(\frac{m}{2},\gamma\right)\partial_\gamma L\left(\frac{n}{2},\gamma\right)\right]\\ &\times\left[\frac{\partial_\gamma L(\frac{n}{2},\gamma)}{L^2(\frac{n}{2},\gamma)}\left(\frac{L(\frac{m}{2},\gamma)}{L(\frac{n}{2},\gamma)}\right)^{\frac{m}{n-m}} - \frac{\partial_\gamma L(\frac{m}{2},\gamma)}{L^2(\frac{m}{2},\gamma)}\left(\frac{L(\frac{m}{2},\gamma)}{L(\frac{n}{2},\gamma)}\right)^{\frac{n}{n-m}}\right]\\ &+\frac{m}{2(n-m)}\left(\frac{L(\frac{m}{2},\gamma)}{L(\frac{n}{2},\gamma)}\right)^{\frac{m}{n-m}}\partial^2_\gamma L\left(\frac{n}{2},\gamma\right) - \frac{n}{2(n-m)}\left(\frac{L(\frac{m}{2},\gamma)}{L(\frac{n}{2},\gamma)}\right)^{\frac{m}{n-m}}\partial^2_\gamma L\left(\frac{m}{2},\gamma\right),\end{aligned} \tag{C2}$$

leading to the simple condition for the minimum through the first derivative

$$nL\left(\frac{n}{2},\gamma\right)\partial_\gamma L\left(\frac{m}{2},\gamma\right) - mL\left(\frac{m}{2},\gamma\right)\partial_\gamma L\left(\frac{n}{2},\gamma\right) = 0. \tag{C3}$$

Here we define $\partial_x f(x) = \partial f(x)/\partial x$. For (C2) we require the derivatives $\partial_\gamma L(s,\gamma)$ and $\partial^2_\gamma L(s,\gamma)$. which involves derivatives of the Bessel function $K_s(a\gamma)$. We need only the first derivative as we can use the two formulas

$$\begin{aligned}\partial_x K_{s-1}(x) &= -K_s(x) + \frac{(s-1)}{x}K_{s-1}(x),\\ \partial_x K_s(x) &= -K_{s-1}(x) - \frac{s}{x}K_s(x).\end{aligned} \tag{C4}$$

We rewrite Eq. (50) in the following short-hand notation:

$$L(s,\gamma) = A_s + B_s\gamma^{2-2s} + C_s\gamma^{1-s}\sum_{k,N\in\mathbb{N}}[d_{skN}K_{s-1}(w_{kN}\gamma) + f_{skN}K_{s-1}(v_{kN}\gamma)] \tag{C5}$$

with the coefficients

$$A_s = 6\zeta(s)\,L_{-3}(s), \quad B_s = \frac{4^s\pi}{\sqrt{3}(s-1)}\zeta(2s-2), \quad C_s = \frac{4}{\sqrt{3}}\frac{(2\pi)^s}{\Gamma(s)},$$
$$d_{skN} = u_2(N)\left(\frac{N}{3k^2}\right)^{(s-1)/2}, \quad f_{skN} = \cos\left(\frac{2\pi N}{3}\right)u_2(N)\left(\frac{N}{3\left(k-\frac{1}{2}\right)^2}\right)^{(s-1)/2}, \tag{C6}$$
$$w_{kN} = \frac{4\pi}{\sqrt{3}}k\sqrt{N}, \quad v_{kN} = \frac{4\pi}{\sqrt{3}}\left(k-\frac{1}{2}\right)\sqrt{N}.$$

The lattice sum derivatives are derived as

$$\partial_\gamma L(s,\gamma) = 2(1-s)B_s\gamma^{1-2s} - C_s\gamma^{1-s}\sum_{k,N\in\mathbb{N}}\left[d_{skN}w_{kN}K_s(w_{kN}\gamma) + f_{skN}v_{kN}K_s(v_{kN}\gamma)\right] \tag{C7}$$

and

$$\partial_\gamma^2 L(s,\gamma) = (2s-1)(2s-2)B_s\gamma^{-2s} + C_s\gamma^{1-s}\sum_{k,N\in\mathbb{N}}\left[d_{skN}w_{kN}^2K_{s-1}(w_{kN}\gamma) + f_{skN}v_{kN}^2K_{s-1}(v_{kN}\gamma)\right]$$
$$+ C_s(2s-1)\gamma^{-s}\sum_{k,N\in\mathbb{N}}\left[d_{skN}w_{kN}K_s(w_{kN}\gamma) + f_{skN}v_{kN}K_s(v_{kN}\gamma)\right]. \tag{C8}$$

We note that Eq. (D1) is converging very fast in our case and only few iterations are required. For example, starting with $\gamma_1 = \sqrt{\frac{8}{3}}$ we get after the first iteration $\gamma_2 = 1.6327632935$ very close to the converged result of $\gamma_2 = 1.6327633049$.

Finally, calculating the (m,n) combination $(n,m\in\mathbb{R})$ reaching the ideal $\gamma_{\rm hcp} = \sqrt{\frac{8}{3}}$ value (see Fig. 8), we use again the Newton-Raphson method in the following form:

$$m_{i+1} = m_i - \frac{\partial_\gamma E^*_{nm}(\gamma_{\rm hcp})}{\partial_m\partial_\gamma E^*_{nm}(\gamma_{\rm hcp})}, \tag{C9}$$

for a fixed n value where $\partial_\gamma E^*_{nm}(\gamma_{\rm hcp})$ is obtained from (C7) and the derivative with respect to m in the denominator is obtained numerically through a two-point formula.

APPENDIX D: MINIMUM OF LENNARD-JONES POTENTIALS WITH RESPECT TO THE LATTICE PARAMETER *a*

We seek for the lattice constant a at fixed c which minimizes the cohesive energy $E^{\rm coh}_{\rm LJ}(n,m,a,c)$. For this we use again the iterative Newton-Raphson algorithm,

$$a_{i+1} = a_i - \frac{\partial_a E^{\rm coh}_{\rm LJ}(a_i,c)}{\partial_a^2 E^{\rm coh}_{\rm LJ}(a_i,c)}, \tag{D1}$$

to obtain the lattice constant a for a specific (n,m,c) combination. As we have $\gamma = c/a$, we can apply the chain rule for the lattice sum, which yields the simple expressions

$$\partial_a L\left(\frac{n}{2},\gamma\right) = -ca^{-2}\partial_\gamma L\left(\frac{n}{2},\gamma\right) \quad \text{and} \quad \partial_a^2 L\left(\frac{n}{2},\gamma\right) = c^2a^{-4}\partial_\gamma^2 L\left(\frac{n}{2},\gamma\right) + 2ca^{-3}\partial_\gamma L\left(\frac{n}{2},\gamma\right), \tag{D2}$$

and we can use the expressions (C7) and (C7) in Appendix C. From this we get the derivatives for the cohesive energy,

$$\partial_a E^{\rm coh}_{\rm LJ}(a,c) = -\frac{m}{2(n-m)}a^{-n-1}\left[nL\left(\frac{n}{2},\gamma\right) + \gamma\partial_\gamma L\left(\frac{n}{2},\gamma\right)\right]$$
$$+\frac{n}{2(n-m)}a^{-m-1}\left[mL\left(\frac{m}{2},\gamma\right) + \gamma\partial_\gamma L\left(\frac{m}{2},\gamma\right)\right] \tag{D3}$$

and

$$\partial_a^2 E^{\rm coh}_{\rm LJ}(a,c) = \frac{m}{2(n-m)}a^{-n-2}\left[n(n+1)L\left(\frac{n}{2},\gamma\right) + (n+2)\gamma\partial_\gamma L\left(\frac{n}{2},\gamma\right) + \gamma^2\partial_\gamma^2 L\left(\frac{n}{2},\gamma\right)\right]$$
$$-\frac{n}{2(n-m)}a^{-m-2}\left[m(m+1)L\left(\frac{m}{2},\gamma\right) + (m+2)\gamma\partial_\gamma L\left(\frac{m}{2},\gamma\right) + \gamma^2\partial_\gamma^2 L\left(\frac{m}{2},\gamma\right)\right]. \tag{D4}$$

APPENDIX E: THE HCP LATTICE SUM EXPRESSED IN QUADRATIC FORMS

In order to show that the lattice sum (14) can be decomposed into four sums containing pure quadratic forms, we start with the double sum $g_1(s,a)$ defined by

$$g_1(s,a)=\sum_{i,j\in\mathbb{Z}}((3i+1)^2+(3i+1)(3j+1)+(3j+1)^2+a^2)^{-s}, \tag{E1}$$

where a and s are real numbers and $s>1$. We will need the following alternative expression for $g_1(s,a)$.

Lemma E.1. The following identity holds:

$$g_1(s,a)=\frac{1}{2}\left(\sum_{i,j\in\mathbb{Z}}{}'(3i^2+9ij+9j^2+a^2)^{-s}-\sum_{i,j\in\mathbb{Z}}{}'(9i^2+9ij+9j^2+a^2)^{-s}\right), \tag{E2}$$

where the primes indicate that the terms corresponding to $(i,j)=(0,0)$ are omitted from the summations if $a=0$.

Proof. First, let us consider the case $a\neq 0$. For $r\in\{0,1,2\}$ let $g_r(s,a)$ be defined by

$$g_r(s,a)=\sum_{i,j\in\mathbb{Z}}[(3i+r)^2+(3i+r)(3j+r)+(3j+r)^2+a^2]^{-s} \tag{E3}$$

and observe that this definition is consistent with (E1) when $r=1$. Then

$$g_0(s,a)+g_1(s,a)+g_2(s,a)=\sum_{\substack{i,j\in\mathbb{Z}\\ i-j\equiv 0\ (\mathrm{mod}3)}}(i^2+ij+j^2+a^2)^{-s},$$

where the sum is over all integers i and j satisfying the given congruence. Since $i-j$ is a multiple of 3, put $i=j+3k$ to get

$$\begin{aligned}g_0(s,a)+g_1(s,a)+g_2(s,a)&=\sum_{j,k\in\mathbb{Z}}[(j+3k)^2+(j+3k)j+j^2+a^2]^{-s}\\&=\sum_{j,k\in\mathbb{Z}}(3j^2+9jk+9k^2+a^2)^{-s}.\end{aligned} \tag{E4}$$

Next, by replacing the summation indices i and j in the definition (E1) with $-i-1$ and $-j-1$, respectively, we readily find that $g_1(s;a)=g_2(s;a)$. Hence, (E4) may be written as

$$\begin{aligned}g_1(s,a)&=\frac{1}{2}\left(\sum_{i,j\in\mathbb{Z}}(3i^2+9ij+9j^2+a^2)^{-s}-g_0(s;a)\right)\\&=\frac{1}{2}\left(\sum_{i,j\in\mathbb{Z}}(3i^2+9ij+9j^2+a^2)^{-s}-\sum_{i,j\in\mathbb{Z}}(9i^2+9ij+9j^2+a^2)^{-s}\right).\end{aligned} \tag{E5}$$

This proves the result in the case $a\neq 0$.

On separating out the terms corresponding to $(i,j)=(0,0)$ from each of the series in (E5), we obtain

$$\begin{aligned}g_1(s,a)&=\frac{1}{2}\left(\frac{1}{a^{2s}}+\sum_{i,j\in\mathbb{Z}}{}'(3i^2+9ij+9j^2+a^2)^{-s}\right)-\frac{1}{2}\left(\frac{1}{a^{2s}}+\sum_{i,j\in\mathbb{Z}}{}'(9i^2+9ij+9j^2+a^2)^{-s}\right)\\&=\frac{1}{2}\sum_{i,j\in\mathbb{Z}}{}'(3i^2+9ij+9j^2+a^2)^{-s}-\frac{1}{2}\sum_{i,j\in\mathbb{Z}}{}'(9i^2+9ij+9j^2+a^2)^{-s}.\end{aligned}$$

This has been obtained under the assumption $a\neq 0$. Now take the limit as $a\to 0$ on each side to complete the proof. This completes the proof of Lemma (E.1)

We will now show that the triple sum $L^B(s,\gamma)$ in (14) can be evaluated in terms of the sums $L(s,\gamma)$ and $M(s,\gamma)$ defined by

$$L(s,\gamma)=L^A(s,\gamma)=\sum_{i,j,k\in\mathbb{Z}}{}'(i^2+ij+j^2+\gamma^2k^2)^{-s} \tag{E6}$$

and

$$M(s,\gamma)=\sum_{i,j,k\in\mathbb{Z}}{}'\left(\frac{i^2}{3}+ij+j^2+\gamma^2k^2\right)^{-s}, \tag{E7}$$

where the primes indicate that the terms corresponding to $(i,j,k)=(0,0,0)$ are omitted from the summations.

Theorem E.2. The following evaluation holds:

$$L^B(s,\gamma) = \frac{1}{2}\Big[M\Big(s,\frac{\gamma}{2}\Big) - L\Big(s,\frac{\gamma}{2}\Big) - M(s,\gamma) + L(s,\gamma)\Big]. \tag{E8}$$

Proof. Let

$$L^C(s,\gamma) = \sum_{i,j,k\in\mathbb{Z}}\left[\Big(i+\frac{1}{3}\Big)^2 + \Big(i+\frac{1}{3}\Big)\Big(j+\frac{1}{3}\Big) + \Big(j+\frac{1}{3}\Big)^2 + \gamma^2k^2\right]^{-s}. \tag{E9}$$

Clearly,

$$L^B(s,\gamma) + L^C(s,\gamma) = \sum_{i,j,k\in\mathbb{Z}}\left[\Big(i+\frac{1}{3}\Big)^2 + \Big(i+\frac{1}{3}\Big)\Big(j+\frac{1}{3}\Big) + \Big(j+\frac{1}{3}\Big)^2 + \gamma^2\Big(\frac{k}{2}\Big)^2\right]^{-s} = L^C\Big(s;\frac{\gamma}{2}\Big),$$

and therefore

$$L^B(s,\gamma) = L^C\Big(s,\frac{\gamma}{2}\Big) - L^C(s,\gamma). \tag{E10}$$

We now turn to the evaluation of $L^C(s,\gamma)$. By definition (E9) we have

$$\begin{aligned} L^C(s,\gamma) &= \sum_{k\in\mathbb{Z}}\left\{\sum_{i,j\in\mathbb{Z}}\left[\Big(i+\frac{1}{3}\Big)^2 + \Big(i+\frac{1}{3}\Big)\Big(j+\frac{1}{3}\Big) + \Big(j+\frac{1}{3}\Big)^2 + \gamma^2k^2\right]^{-s}\right\} \\ &= 3^{2s}\sum_{k\in\mathbb{Z}}\left\{\sum_{i,j\in\mathbb{Z}}[(3i+1)^2 + (3i+1)(3j+1) + (3j+1)^2 + 9\gamma^2k^2]^{-s}\right\} \\ &= 3^{2s}\sum_{k\in\mathbb{Z}} g_1(s;3\gamma k), \end{aligned}$$

where in the last step we used the definition of g_1 from (E1). Now apply Lemma E.1 to get

$$\begin{aligned} L^C(s,\gamma) &= 3^{2s}\sum_{k\in\mathbb{Z}}\left[\frac{1}{2}\sum_{k\in\mathbb{Z}}(3i^2+9ij+9j^2+9\gamma^2k^2)^{-s} - \frac{1}{2}\sum_{k\in\mathbb{Z}}(9i^2+9ij+9j^2+9\gamma^2k^2)^{-s}\right] \\ &= \frac{1}{2}[M(s,\gamma) - L(s;\gamma)]. \end{aligned} \tag{E11}$$

On using (E11) in (E10) we complete the proof of Theorem (E.2).

Adding both lattice sums (12) and (14) and using (E8) we get

$$L^{\mathrm{hcp}}(s,\gamma) = L^A(s,\gamma) + L^B(s,\gamma) = \frac{1}{2}\Big[M\Big(s,\frac{\gamma}{2}\Big) - L\Big(s,\frac{\gamma}{2}\Big) - M(s,\gamma) + 3L(s,\gamma)\Big]. \tag{E12}$$

This can be simplified even further, as follows. On replacing the summation index i with $i+j$ in (E6) we obtain

$$\begin{aligned} L(s,\gamma) &= {\sum_{i,j,k\in\mathbb{Z}}}'(i^2+ij+j^2+\gamma^2k^2)^{-s} = {\sum_{i,j,k\in\mathbb{Z}}}'[(i+j)^2+(i+j)j+j^2+\gamma^2k^2]^{-s} \\ &= {\sum_{i,j,k\in\mathbb{Z}}}'(i^2+3ij+3j^2+\gamma^2k^2)^{-s} = 3^{-s}{\sum_{i,j,k\in\mathbb{Z}}}'\Big(\frac{i^2}{3}+ij+j^2+\frac{\gamma^2k^2}{3}\Big)^{-s} = 3^{-s}M\Big(s,\frac{\gamma}{\sqrt{3}}\Big), \end{aligned} \tag{E13}$$

or equivalently $M(s,\gamma) = 3^sL(s,\gamma\sqrt{3})$. On using this in (E12) we deduce that the lattice sum for the hcp structure can be expressed in terms of the sole function $L(s,\gamma)$ by

$$L^{\mathrm{hcp}}(s,\gamma) = \frac{3^s}{2}\left[L\Big(s,\frac{\gamma\sqrt{3}}{2}\Big) - L(s,\gamma\sqrt{3})\right] + \frac{1}{2}\Big[3L(s,\gamma) - L\Big(s,\frac{\gamma}{2}\Big)\Big], \tag{E14}$$

where $L(s,\gamma)$ is given by (E6). Equation (E14) is the generalized form of the quadratic equation for the ideal hcp lattice sum ($\gamma = \sqrt{\frac{8}{3}}$) introduced in [20]. Table IV contains the lattice sums for a few selected values of s and γ. We note that the decomposition into quadratic forms is numerically less stable at higher s and smaller γ values as large terms cancel out in the sum (E12).

TABLE IV. Values for $L(s,\gamma)$, $L(s,\gamma\sqrt{3})$, $L(s,\gamma\sqrt{3}/2)$, and $L(s,\gamma/2)$ are calculated using (32) and checked using (38). The values for $L_B(s,\gamma)$ are calculated using (43) and checked using (49). Finally, the values of $L^{\rm hcp}(s,\gamma)$ are calculated using (15) and checked using (E14); that is, $L^{\rm hcp}(s,\gamma) = L_A(s,\gamma) + L_B(s,\gamma) = \frac{3^s}{2}[L(s,\frac{\gamma\sqrt{3}}{2}) - L(s,\gamma\sqrt{3})] + \frac{1}{2}[3L(s,\gamma) - L(s,\frac{\gamma}{2})]$. All calculations have been confirmed to at least 20 significant figures, and the results have been rounded to 15 significant figures.

Term	$s=2$	$s=3$	$s=6$
$\gamma = \sqrt{\frac{8}{3}}$			
$L_A(s,\gamma) = L(s,\gamma)$	12.1870358329088	6.92865992678971	6.02086135277707
$L_B(s,\gamma)$	13.1520465051463	7.52623735105191	6.11143241632185
$L(s,\gamma\sqrt{3})$	9.20293595374102	6.43722899163756	6.00985825575242
$L(s,\gamma\sqrt{3}/2)$	13.6814750856921	7.36211367799812	6.05865169246628
$L(s,\gamma/2)$	26.1897950101762	16.8480717564210	29.3684118845362
$L^{\rm hcp}(s,\gamma)$	25.3390823380551	14.4548972778416	12.1322937690989
$\gamma = \frac{2}{3}$			
$L_A(s,\gamma) = L(s,\gamma)$	36.9809850738719	35.1941483523189	266.925005360286
$L_B(s,\gamma)$	52.5108713421994	75.6309688124675	780.320419437853
$L(s,\gamma\sqrt{3})$	16.6903918205456	8.63749904269048	6.44289177567726
$L(s,\gamma\sqrt{3}/2)$	49.5097759230495	68.7579632615801	1466.59547705827
$L(s,\gamma/2)$	227.333699312008	1507.18474463740	1063157.51883750
$L^{\rm hcp}(s,\gamma)$	89.4918564160713	110.825117164786	1047.24542479814
$\gamma = 2$			
$L_A(s,\gamma) = L(s,\gamma)$	10.6947526881655	6.62129785066350	6.01123767234242
$L_B(s,\gamma)$	8.89689023466853	3.56318127956155	1.11454282050704
$L(s,\gamma\sqrt{3})$	8.70567252140502	6.40314706955824	6.00981976517265
$L(s,\gamma\sqrt{3}/2)$	11.6894842922333	6.81240163025634	6.01588343941374
$L(s,\gamma/2)$	19.7552781562826	10.5448084303891	8.20257055308643
$L^{\rm hcp}(s,\gamma)$	19.5916429228340	10.1844791302250	7.12578049284946

[1] T. C. Hales, in *The Kepler Conjecture: The Hales-Ferguson Proof*, edited by J. C. Lagarias (Springer, New York, 2011), pp. 65–82.
[2] T. C. Hales, Ann. Math. **162**, 1065 (2005).
[3] W. Barlow, Nature (London) **29**, 205 (1883).
[4] P. Krishna, D. Pandey, and C. A. Taylor, *Close-Packed Structures* (International Union of Crystallography, Chester, UK, 1981).
[5] C. H. Loach and G. J. Ackland, Phys. Rev. Lett. **119**, 205701 (2017).
[6] G. Osang, H. Edelsbrunner, and M. Saadatfar, Soft Matter **17**, 9107 (2021).
[7] J. E. Jones, Proc. R. Soc. London A **106**, 709 (1924).
[8] J. E. Jones and A. E. Ingham, Proc. R. Soc. London A **107**, 636 (1925).
[9] E. Grüneisen, Ann. Phys. **344**, 257 (1912).
[10] T. Kihara and S. Koba, J. Phys. Soc. Jpn. **7**, 348 (1952).
[11] R. E. Crandall and J. F. Delord, J. Phys. A: Math. Gen. **20**, 2279 (1987).
[12] J. M. Borwein, M. Glasser, R. McPhedran, J. Wan, and I. Zucker, *Lattice Sums Then and Now* (Cambridge University Press, Cambridge, 2013).
[13] I. J. Zucker, J. Phys. A **7**, 1568 (1974).
[14] A. Burrows, S. Cooper, and P. Schwerdtfeger, Proc. R. Soc. A. **478**, 20220334 (2022).
[15] A. Burrows, S. Cooper, and P. Schwerdtfeger, arXiv:2105.08922 [math-ph] (2021).
[16] G. Kane and M. Goeppert-Mayer, J. Chem. Phys. **8**, 642 (1940).
[17] R. Bell and I. Zucker, in *Rare Gas Solids*, edited by M. L. Klein and J. A. Venebles (Academic, New York, 1976), Vol. 1, pp. 122–171.
[18] P. Schwerdtfeger, N. Gaston, R. P. Krawczyk, R. Tonner, and G. E. Moyano, Phys. Rev. B **73**, 064112 (2006).
[19] F. H. Stillinger, J. Chem. Phys. **115**, 5208 (2001).
[20] A. Burrows, S. Cooper, E. Pahl, and P. Schwerdtfeger, J. Math. Phys. **61**, 123503 (2020).
[21] E. Florez, O. Smits, J.-M. Mewes, P. Jerabek, and P. Schwerdtfeger, J. Chem. Phys. **157**, 064304 (2022).
[22] P. Epstein, Math. Ann. **56**, 615 (1903).
[23] T. M. Middlemas, F. H. Stillinger, and S. Torquato, Phys. Rev. E **99**, 022111 (2019).
[24] L. Kantorovich, *Quantum Theory of the Solid State: An Introduction* (Springer Science & Business Media, Berlin, 2004).
[25] A. A. Terras, Trans. Amer. Math. Soc. **183**, 477 (1973).
[26] I. J. Zucker and M. M. Robertson, J. Phys. A: Math. Gen. **8**, 874 (1975).
[27] P. Schwerdtfeger, A. Burrows, and O. R. Smits, J. Phys. Chem. A **125**, 3037 (2021).
[28] A. Burrows, S. Cooper, and P. Schwerdtfeger, Phys. Rev. E **104**, 035306 (2021).
[29] R. Howard, Phys. Lett. A **32**, 37 (1970).
[30] R. A. Aziz, J. Chem. Phys. **99**, 4518 (1993).

[31] P. Schwerdtfeger, R. Tonner, G. E. Moyano, and E. Pahl, Angew. Chem. Int. Ed. **55**, 12200 (2016).
[32] R. E. Crandall, Exper. Math. **8**, 367 (1999).
[33] A. Kratzer, Z. Phys. **3**, 289 (1920).
[34] O. Emersleben, Mathematische Nachrichten **4**, 468 (1950).
[35] I. J. Zucker, J. Phys. A **8**, 1734 (1975).
[36] Y. A. Freiman, S. M. Tretyak, A. Grechnev, A. F. Goncharov, J. S. Tse, D. Errandonea, H.-k. Mao, and R. J. Hemley, Phys. Rev. B **80**, 094112 (2009).
[37] A. Dewaele, A. D. Rosa, N. Guignot, D. Andrault, J. E. F. S. Rodrigues, and G. Garbarino, Sci. Rep. **11**, 15192 (2021).
[38] U. Häussermann and S. I. Simak, Phys. Rev. B **64**, 245114 (2001).
[39] P. Schwerdtfeger and A. Burrows, Program Jones—A Fortran program for SC, BCC, FCC, and HCP lattice sums, Massey University, Auckland, http://ctcp.massey.ac.nz (2021).
[40] G. E. Andrews, R. Askey, and R. Roy, *Special Functions*, Encycl. Math. Appl. Vol. 71 (Cambridge University Press, Cambridge, 1999).
[41] N. M. Temme, *Special Functions: An Introduction to the Classical Functions of Mathematical Physics* (John Wiley & Sons, 1996).
[42] J. M. Borwein and P. B. Borwein, Trans. Am. Math. Soc. **323**, 691 (1991).
[43] S. Cooper, *Ramanujan's Theta Functions* (Springer, Berlin, 2017).
[44] S. Cooper, J. Comput. Appl. Math. **160**, 77 (2003).
[45] T. M. Apostol, *Introduction to Analytic Number Theory* (Springer Science & Business Media, Berlin, 1998).
[46] G. Hämmerlin and K.-H. Hoffmann, *Numerical Mathematics* (Springer Science & Business Media, Berlin, 2012).